URANIUM EXTRACTION BY COMPLEXATION WITH SIDEROPHORES

by

Cristina Bahamonde Castro

A thesis submitted to the faculty of
The University of Utah
in partial fulfillment of the requirements for the degree of

Master of Science

in

Nuclear Engineering

Department of Civil and Environmental Engineering

The University of Utah

August 2015

The University of Utah Graduate School

STATEMENT OF THESIS APPROVAL

The thesis of **Cristina Bahamonde Castro**

has been approved by the following supervisory committee members:

Luther W. McDonald IV	, Chair	**06/11/2015** Date Approved
Terry A. Ring	, Member	**06/11/2015** Date Approved
Azaree T. Lintereur	, Member	**06/11/2015** Date Approved

and by **Michael E. Barber** , Chair/Dean of

the Department/College/School of **Civil and Environmental Engineering**

and by David B. Kieda, Dean of The Graduate School.

ABSTRACT

One of the major concerns of energy production is the environmental impact associated with the extraction of natural resources. Nuclear energy fuel is obtained from uranium, an abundant and naturally occurring element in the environment, but the currently used techniques for uranium extraction leave either a significant fingerprint (open pit mines) or a chemical residue that alters the pH of the environment (acid or alkali leaching). It is therefore clear that a new and greener approach to uranium extraction is needed. Bioleaching is one potential alternative. In bioleaching, complexants naturally produced from fungi or bacteria may be used to extract the uranium. In the following research, the siderophore enterobactin, which is naturally produced by bacteria to extract and solubilize iron from the environment, is evaluated to determine its potential for complexing with uranium.

To determine whether enterobactin could be used for uranium extraction, its acid dissociation and its binding strength with the metal of interest must be determined. Due to the complexity of working with radioactive materials, lanthanides were used as analogs for uranium. In addition, polyprotic acids were used as structural and chemical analogs for the siderophore during method development. To evaluate the acid dissociation of enterobactin and the subsequent binding constants with lanthanides, three different analytical techniques were studied including: potentiometric titration, UltraViolet Visible (UV-Vis) spectrophotometry and Isothermal Titration Calorimetry (ITC).

After evaluation of three techniques, a combination of ITC and potentiometric titrations was deemed to be the most viable way for studying the siderophore of interest.

The results obtained from these studies corroborate the ideal pH range for enterobactin complexation to the lanthanide of interest and pave the way for determining the strength of complexation relative to other naturally occurring metals. Ultimately, this fundamental research enhances our current understanding of heavy metal complexation to naturally occurring complexants, which may enhance the metals mobility in the environment or potentially be used as a greener alternative in uranium extraction or remediation.

TABLE OF CONTENTS

LIST OF TABLES

LIST OF FIGURES

CHAPTER 1

INTRODUCTION

Changing the way natural resources are exploited to produce energy can radically minimize the environmental impact of energy production in the world, which has been a subject of great concern in the last decades. Nuclear energy has been in a resurgence the past few years with many new plants under construction and many more planned. The primary fuel for nuclear power is uranium, which is an abundant and naturally occurring element in nature. The complex chemistry of uranium enables it to exist in multiple forms in the environment. In total, it is estimated that there is 16.2 million tons of uranium stored in earth's crust [1]. These resources are often classified in high cost (more than USD $130/kg Uranium) and low cost (less than USD $130/kg Uranium).

1.1 Uranium extraction techniques

Three techniques can be used for uranium mining: open-pit mining, underground mining, and in situ leaching (acid or alkali) [2]. In some cases, methods that produce uranium as a by-product can also contribute significantly to the amount of metal mined, but since these techniques were not specifically designed for uranium extraction, they will not be further explained. The most convenient and economical extraction method is chosen based on the size, grade, depth, and geology of the ore.

Underground mining is the most common method of extracting uranium both in high cost and low cost uranium mines. Open-pit mining is the second biggest contributor in high cost mines, and in situ leaching (more specifically acid leaching) is the second biggest contributor in low cost mines [1].

Underground mining is used for deeper uranium deposits or deposits where the size, shape or orientation of the ore permit more cost-effective underground mining. Depending on several factors, the following excavation techniques may be used:

a) Longwall Retreat: The rock that contains the ore is removed in one step and the remaining space is either filled with debris or allowed to collapse,
b) Room and Pillar: Natural pillars are left intact in the mining process so that the mined rooms do not collapse, or
c) Panels: The mine is divided into sections surrounded by solid strata and only the necessary roads are built to get to the ore bearing rocks.

Both the ore of interest and the waste rock generated during mining are usually removed using shafts and elevators or carried to the surface in trucks.

Open-pit mining or surface mining uses open excavations to mine to the desired ore. Therefore, this technique is mainly used for deposits that are located near the surface. The excavations are usually broad on the surface and narrow with increasing depth. Normally, lower-grade ores are recovered with this method as open-pit is more cost effective than underground mining. Waste materials generate the largest share of cost in open pit mining. Hence, a lot of delineation of the deposit and computer modelling are needed before the mining process starts [3]. Normally, top soil is saved to reuse later in the restoration process and the rest of the extracted rock between top soil and the ore is returned

to mined-out areas during mining to reduce transportation costs. Once the ore is exposed, radiometric probing is used to define the dimensions of the ore but usually parts of the ore that are delineated by drilling cannot be mined using open-pit methods and underground mines may be developed from the pit bottom to recover them. In both underground and open-pit mining, the extracted ore is piled at the surface or taken directly to a processing mill that can be at the mine or at some centralized location. This so-called milling and the subsequent leaching during this processing get the uranium out of the ore using chemical reactions with aggressive reagents such as sulfuric acid.

In situ leaching, as opposed to the previously presented physical methods, uses chemical reactions to extract uranium from the ores. In situ leaching is used when one or more of the following conditions exist:

a) the ore is too deep to be mined on a budget using physical methods,
b) the ore is below the water table,
c) methane and hydrogen disulfide are associated with the ore in high amounts,
d) the ore grade is low,
e) the ore is too thin to be mined by physical methods and/or
f) a highly permeable rock formation exists in which uranium can be economically produced.

During in situ leaching, a solvent, also called lixiviant, is injected using drilled conduits underground which pass through the uranium ore. The solvent for in situ mining is generally composed of water containing added oxygen and carbon dioxide or sodium bicarbonate. The oxygen, carbon dioxide and sodium bicarbonate aid in mobilizing the uranium. After contacting the ore, this solution is pumped back to the surface and the

uranium is extracted using ion exchange or solvent extraction. The ion exchange process employs a resin that is first fully saturated with uranium and then flushed with a highly concentrated salt solution, which releases uranium into the solution. The solvent extraction process is based on the unmixable properties between the leach solution and the uranium solute, where the solvents used are organic compounds that can combine with cationic or anionic solutes.

All currently used techniques for uranium extraction leave a significant fingerprint and a chemical residue that alters the pH of the environment. Table 1-1 shows a summary of the environmental impact of each technique.

1.2 Bioleaching

Provided the high environmental impact of all the conventional techniques, a potential greener alternative that could be used is bioleaching [4]. Bioleaching is primarily used for metal extraction from low-grade ores where the metal is found in insoluble forms like oxides. To extract the metal, anions produced from microorganism, such as fungi and bacteria, serve as complexants to mobilize the uranium [5]. One of the most useful complexants to extract trivalent metals are siderophores, which will be extensively explained in a following section. Although siderophores can be produced from fungi or bacteria, this study will use enterobactin, a siderophore from *Escherichia coli* and for this reason, only bioleaching with bacteria will be discussed.

Bioleaching is nowadays used to extract uranium, copper and gold primarily on an industrial scale, and in situ leaching is the preferred method of contact between the ore and the bacteria [4]. Nonetheless, there are other methods like dump leaching, tank leaching,

and heap leaching. In addition to metal mining, it is important to note that due to the nature of the process, bioleaching can also be used for other potential environmentally friendly applications such as metal recovery from waste or heavy metal remediation processes.

Depending on whether the bacteria cell directly oxidizes the metal or if it produces a lixiviant that chemically oxidizes the metal, bioleaching can be classified as direct or indirect, respectively. In the specific case of uranium ores, bioleaching is known as a two-step process. First, pyrite is used for indirect leaching to help the preliminary uranium solubilization. Second, direct leaching is achieved between the complexant and the metal [6]. The reactions involved in this process can be seen in Figure 1-1, where the continuous lines indicate the reactions catalyzed by the bacteria. Several factors are known to influence the bioleaching process, some of them regarding the optimal bacteria growth like the nutrients and the oxygen conditions in the bacteria's environment, and other factors regarding the chemical process, such as the pH of the environment and the temperature. These last two factors are key to the metals' solubilization and therefore, even in optimal bacterial conditions, special attention should be paid to them.

From an economical point of view, the operating costs of bioleaching are much lower than for most conventional hydrometallurgical processes because most of the cost of the traditional processes is due to the first steps required to obtain the solution containing the metal. Since the processing can be built right next to the ores, transport costs are also greatly reduced. Although it is important to ensure longer contact times for uranium solubilization than in traditional methods, and even though certain factors such as the pH or the temperature should be controlled, the process is still easier to control and execute than traditional processes (since the microorganisms involved can grow and complex in

highly acidic environments with a high heavy metal content). For these reasons, further development of bioleaching will be of great interest in the future.

In the present work, siderophores, which are the naturally produced lixiviants from bacteria to extract and solubilize iron from the environment, are evaluated to determine their potential for complexing with uranium. Uranium is present in very different forms in ores due to its versatile chemistry, but not all these ores are equally suitable for bioleaching. From all the different uranium ores found in the environment, pitchblende and uraninite are of particular economic importance, as they contain crystalline forms of UO_2 in vein deposits and a high pyrite content. Table 1-2 shows a summary of the different uranium ores, their chemical composition and their degree of suitability for bioleaching. In general, it is possible to say that oxides, phosphates, sulphates and carbonates can be solubilized easier than silicates.

Although commercial applications of bioleaching of uranium have been reported since the 1960s [7], the siderophore enterobactin, which is common and highly available in nature, has never been evaluated regarding its complexation potential with uranium. Other microbial systems have been extensively studied [8]. Knowledge of siderophores and other potential environmental interferences to bioleaching is important to determine the best process that could be commercially scaled. For instance, the presence of unwanted yeast or fungi in the environment of the ore can represent a competitive participation in the consumption of oxygen and secretion of organic compounds. Table 1-3 shows a summary of the different microorganisms typically used for uranium extraction. Their characteristics and the requirements for bioleaching to take place were determined by carrying out in-depth studies of the influence of the different variables such as pH, temperature and others

[9].

1.3 Chosen complexants: siderophores

The main complexant chosen for this study is enterobactin, a siderophore from *Escherichia coli*. Even though siderophores are typically produced by microorganisms to scavenge iron from the environment, previous studies have shown that siderophores with certain chemical groups such as carboxylates, can complex with uranium, and some siderophores also have been proven to have a higher selectivity for uranium [10] [11]. In general, siderophores may be characterized as low molecular weight compounds (approximately 1 kDa) with high affinity and selectivity for iron (III) [12]. They are synthesized according to the different iron levels of the environment in which the organism lives, therefore, around 500 different types of siderophores are believed to exist. The majority of siderophores fall under catecholate or hydroxamate types. While bacteria produces many different types of siderophores, most fungi produce hydroxamate type siderophores, with a couple of exceptions like the polycarboxylate type rhizoferrin.

All organisms need iron to live, mainly because iron has an ideal chemistry for metabolic processes and electron transport ($Fe^{II} \rightleftarrows Fe^{III} \rightleftarrows Fe^{IV}$). In addition, iron is also able to coordinate and activate oxygen. Even though iron is the second most abundant metal on the planet, it is very insoluble in aerobic environments due to its tendency to form insoluble hydroxides and oxyhydroxides. Therefore, it is necessary for organisms to develop strategies to extract that iron in the needed quantity. As humans use proteins to extract iron from their dietary intake, microorganisms use siderophores to capture and solubilize the iron.

Siderophores have a much higher affinity for iron (III) over iron (II), which ensures that iron (III) will not enter a redox cycle generating damaging radicals. The reason behind this selectively is probably related to the fact that there are more biologically important dipositive cations than tripositive cations. Iron (III) is most likely to bind to the ligand via negatively charged oxygen atoms, so the interaction between iron (III) and the donor atoms is mostly electrostatic, forming an octahedral complex geometry that is the most convenient to optimize the Coulomb interactions [13]. Hexadentate siderophores (having six available positions for binding) are most common in nature due to a concentration effect rather than a chelate effect. The chelate effect is the greater stability of a complex that contains a polydentate ligand compared to the stability of a complex with the same number of monodentate ligands. Whereas the concentration effect refers to the difference when applying the stability constant formula (Equation 1-15), which will be further explained in the next section. Basically, in order to complex to a trivalent metal, three singly charged ligands would be needed or only one triply charged ligand. Therefore, when applying the stability constant formula (Equation 1-15), the singly charged ligand will be to the power of three while the triply charged ligand will be to the power of one. This means less triply charged ligands will be needed and therefore this leads to the conclusion that ligands with multiple binding sites are far more effective as chelators for polyvalent metals than singly charged ligands [14]. To release iron after an iron-siderophore complex has been formed, the coordinated iron reduces back from (III) to (II). For the same reason, siderophores have been found to bind more likely to metals with +3 valence, for example, aluminum [12].

Siderophores have been proved to have different applications apart from metal mining, a subject of interest in this thesis [15]. In medicine, both naturally occurring

siderophores and synthetic siderophore analogues have been studied to treat sicknesses as aluminum overload [16] or thalassemia [17]. In addition, research has been performed on exploiting siderophore uptake systems for drug transport [18] [19], excretion of actinides in contaminated environments, and as potential treatments for cancer, malaria or other infectious diseases [17] [20] [21] [22]. Siderophores have also been used to treat metal pollution coming from motor vehicles, industry and mining [23] [24]. They are particularly effective at mobilizing metals [25] [26], solubilizing actinides [27], and in remediation of waste sites [28] [29] [30]. Finally, siderophores also have an important role in nuclear fuel reprocessing especially in the Plutonium Uranium Redox EXtraction (PUREX process), which uses solvent extraction to separate uranium and plutonium from other fission products that cannot be reused as fuel, such as heavy metals and minor actinides [31] [32].

Additional details on the selected siderophore for this study (enterobactin) and about the current knowledge of its role in metal complexation are presented in Chapter 5 of this thesis.

1.4 The chemistry behind bioleaching

Since bioleaching as a process relies on chemical reactions to extract the metal of interest, a fundamental understanding of the quantitative behavior of the bioleaching complexants is needed. The first step in developing this fundamental understanding is to determine the pK_a values of the complexants as defined in Equation 1-4. With pK_a values, it is possible to calculate the equilibrium concentrations of the different species in solution at a certain pH. These calculations are useful in complexation processes such as bioleaching because knowing the concentration of the different species in solution can help in

predicting the complexes that will form between complexants and metal ions.

In order to understand what happens at a molecular scale in the bioleaching process, the chemistry behind it will be explained in the following section.

All weak acids in solution react donating a proton to water, following the reaction:

$$HA + H_2O \rightleftarrows A^- + H_3O^+ \quad (1\text{-}1)$$

HA is the fully protonated acid, A^- is the deprotonated acid, H_2O is the water medium and H_3O^+ is the form a proton typically adopts in aqueous solutions, better known as the hydronium ion.

Equation 1-1 rewritten can be expressed as:

$$HA \rightleftarrows A^- + H^+ \quad (1\text{-}2)$$

$$K_a = \frac{[A^-][H^+]}{[HA]} \quad (1\text{-}3)$$

Equation 1-3 is the equilibrium constant for the reaction, also called: acid dissociation constant, K_a, which is the ratio between the concentration of the products and the concentration of the reactants. Since weak acids are only partially dissociated in water, their K_a values tend to be small (from 10^{-12} to 100). Strong acids are fully dissociated in water so their values are higher than 100.

K_a is therefore a measurement of the degree of deprotonation of a weak acid in solution. This value can span many orders of magnitude. Hence, the degree of deprotonation can also be expressed using the negative logarithm of K_a.

$$pK_a = -log_{10}\, K_a \quad (1\text{-}4)$$

Weak acids have pK_a values from -2 to 12, while strong acids have values of less than -3. As a practical interpretation, it can be said that the higher the pK_a value, the lower the K_a value, and therefore the lower the dissociation degree of the acid in solution, and

consequently, the more difficult it is for protons to leave the molecule. The lower the pK_a value, the higher the K_a value, the higher the degree of dissociation of the acid in solution and the easier it is for protons to leave the molecule. Following this rationale, in order to capture and solubilize metals, bioleaching complexants should be adequately deprotonated, which means those with low pK_a values (3.5-5) will be more convenient for acid complexation as it will mean the experiments will not have to be performed in extreme pH ranges. This was the criteria used for choosing the complexants for this study, in our case, the siderophore enterobactin and its chemical analogs EDTA (EthyleneDiamineTetraacetic Acid) and HIBA (HydroxyIsoButyric Acid).

It is important to say that Equation 1-3 is a simplification of the actual thermodynamically applicable expression. The thermodynamic equilibrium constant for Equation 1-1 is written as a function of the activities of the compounds in solution:

$$K^{\ominus} = \frac{\{A^-\}\{H_3O^+\}}{\{HA\}\{H_2O\}} \tag{1-5}$$

This expression can also be rewritten as a product of concentrations times activity coefficients as:

$$K^{\ominus} = \frac{[A^-][H_3O^+]}{[HA][H_2O]} \frac{\gamma_{A^-}\gamma_{H_3O^+}}{\gamma_{HA}\,\gamma_{H_2O}} = \frac{[A^-][H_3O^+]}{[HA][H_2O]}\ \Gamma \tag{1-6}$$

Γ is therefore the quotient of activity coefficients. Equation 1-3 applies to ideal solutions and Equation 1-6 to real solutions because the activities depend on the different factors that can alter the chemical potential of the solution, principally temperature and ionic strength. For this reason, every equilibrium constant value is reported and determined at a specific temperature and ionic strength, because when working at a high ionic strength, Γ can be assumed constant, as well as $[H_2O]$ leading to Equation 1-3. It is worth mentioning that other experimental conditions such as pressure also have a thermodynamically

influence in equilibrium constants, but because at a laboratory scale the conditions with a bigger influence in K are ionic strength and temperature, they are the ones that typically require more attention. In order to adjust the ionic strength to a fixed concentration value, a salt that does not interfere and ideally carries ions already involved in the reaction is added. For example, during the experiments carried out in this study, total ionic strength in solution was often adjusted to 0.1 M using a standard salt such as NaCl. To calculate the ionic strength, Equation 1-7 is used:

$$\mu = \frac{1}{2} \sum_{i=1}^{n} [i] z_i{}^2 \tag{1-7}$$

$[i]$ is the concentration of the 'i' ion, and z_i is the ion's charge. Adjusting the ionic strength and working at a fixed temperature makes it possible to use Equation 1-3 to calculate equilibrium constants even in nonideal solutions.

The pK_a values also depend on the molecular structure of the acid, particularly when talking about polyprotic acids (acids that contain more than one ionizable proton). In these acids, a pK_a value can be determined per proton lost, therefore if an acid can lose three protons there will be pK_{a1}, pK_{a2} and pK_{a3} values. The corresponding chemical reactions to these values are shown in Equation 1-8. The different protonation states of the polyprotic acid are called species, and the total concentration of acid accounts for the sum of all the different species' concentrations.

$$H_3A \rightleftarrows H_2A^- + H^+ \rightleftarrows HA^{-2} + 2H^+ \rightleftarrows A^{-3} + 3H^+ \tag{1-8}$$

In this research, only polyprotic acids were used, since the bioleaching complexant chosen for this study, enterobactin, is a polyprotic siderophore. This means that more than one pK_a value was determined and they all needed to be taken into account in the chemical model employed.

In order to control the degree of protonation of a weak acid in solution, the pH of the solution can be used, since dissociation and pH are related through the Henderson-Hasselbach equation (Equation 1-9):

$$pH = pK_a + log_{10}\ \frac{[A^-]}{[HA]} \tag{1-9}$$

The relationship between pH and the degree of protonation may be used to create speciation diagrams. Figure 1-2 shows an example speciation diagram for one of the complexants used in this study, EDTA.

If the pK_a values are available from the literature, and the initial and final concentrations of the complexant are known, then a speciation diagram showing the concentration of each species at the different pH values can be produced. If the pK_a values are not known, then those of a similar compound are often used as an analog [33] [34]. Because the experiments are always done in solution, it is important to also input the self-ionization constant of water for the certain values of ionic strength and temperature selected:

$$K_w = [H_3O^+][OH^-] \tag{1-10}$$

The easiest way to produce speciation diagrams is using HySS software [35], which uses the Newton-Raphson method to iteratively solve a set of equations. Solving these equations yields the concentration of individual species at certain pH value, which is useful in the design of bioleaching experiments as will later be explained. For example, it is essential to know the working pH range in which the complexant is fully or partially deprotonated.

HySS is also able to produce simulated titrations. A more detailed explanation of what titrations consist of and which components are involved in them can be found in

section 1.5 of this chapter. In titration simulations, the concentration of titrant and titrand are input as well as the volumes and concentrations of compounds and pH of each. The software then estimates the volume of equivalence point in the titration. An example for the titration of EDTA is shown in Figure 1-3.

Once the pK_a values have been determined and the speciation diagram has been produced, the next step of bioleaching can take place: the metal-ligand complexation. For these studies, the trivalent lanthanides where used as less hazardous analogs for the actinides. The lanthanides, unlike transition metals, do not form covalent bonds, but rather are bound to complexants through electrostatic bonds. If the metal is, for example, trivalent, it means that it can accept up to three electrons to be on a more stable configuration. As a ligand loses a proton, it will have an extra electron to donate to the metal.

In a complex, the total number of metal atoms compared to the total number of ligand atoms is called metal-ligand ratio. For example, a complex consisting of only one metal and one monodentate ligand will have a 1:1 metal-ligand ratio. The formation of f-element complexes, such as lanthanides, is described by the Eigen-Tamm Mechanism [36], which corresponds to Equation 1-11:

$$M(aq) + L(aq) \overset{1}{\rightarrow} M(aq)L(aq) \overset{2}{\rightarrow} M(H_2O)_nL(aq) \overset{3}{\rightarrow} ML(aq) \qquad (1\text{-}11)$$

In the first step, M(aq)L(aq) forms, and this formation is controlled by diffusion. During this step the metal cation and ligand anion remain fully hydrated. In step two, an outer sphere complex is formed in which the metal cation and ligand anion remain separated by at least one water molecule. In most cases, the reaction will proceed to this third step in which an inner-sphere complex is formed by direct contact between the ligand and the metal cation.

To quantify the strength of the complex formed, an association constant of the complex, also called stability constant is determined. This value is based on the thermodynamics of the reaction, which are described by the change of three main variables: Gibbs free energy (G), enthalpy (H) and entropy (S) of the reaction.

$$\Delta G = \Delta H - T\Delta S \tag{1-12}$$

If the terms add up to a negative Gibbs free energy change, this means the reaction is spontaneous. The reaction is nonspontaneous if the terms add up to a positive change in G. At standard state conditions (i.e., 25 ºC and 1 atm of pressure) it is possible to determine standard state free energy ΔG^0. Once this is known, Gibbs free energy and the concentration of the species in the reaction can be related at any point of the reaction, including at equilibrium ($\Delta G = 0$ and Q=K), as can be seen by using Equation 1-14 where Q is the reaction quotient described in Equation 1-13.

$$A + B \leftrightarrow C + D$$

$$Q = \frac{[C][D]}{[A][B]} \tag{1-13}$$

$$\Delta G = \Delta G^0 - RT \ln Q \tag{1-14}$$

Stability constants are also often represented in terms of the concentration of complex formed versus the concentration of metal and ligand separately. For Equation 1-11 and a complex undergoing the Eigen-Tamm mechanism all the way to the third step, this stability constant would be expressed as:

$$\beta = \frac{[ML(aq)]}{[M(aq)][L(aq)]} \tag{1-15}$$

Because a metal may have more than one ligand surrounding it, leading to a 1:2 complex as explained before, several equations are needed to describe the complexation process:

$$M + L \rightleftarrows ML \tag{1-16}$$

$$K_1 = \frac{[ML]}{[M][L]} \tag{1-17}$$

$$ML + L \rightleftarrows ML_2 \tag{1-18}$$

$$K_2 = \frac{[ML_2]}{[ML][L]} \tag{1-19}$$

K_1 and K_2 are called stepwise constants, and are used to describe the formation of a 1:2 complex. Sometimes, complexes undergo a first step with one metal and one ligand complexing (K_1) and then another ligand complexes with the previous ML complex (K_2). At other times, complexes may directly add two ligands in one step depending on the thermodynamically favorable mode of complexation. To express the stability constant of the overall process starting with only pure metal and pure ligand as the reactants, the stepwise constants can be multiplied for all the steps giving an overall constant (β).

$$\beta_{12} = K_1 K_2 = \frac{[ML_2]}{[M][L]^2} \tag{1-20}$$

It is worth noting that in the case of a 1:1 complex, $\beta_{11} = K_1$. Stability constants are crucial in bioleaching since they quantify the strength of a metal-ligand complex. If the stability constant for a complexant, for example, enterobactin (E), is higher for metal M_1 (β_E:M_1) than for metal M_2 (β_E:M_2), enterobactin will capture M_1 instead of M_2, even if they are both present in the environment.

A similar model can be developed in HySS to include the different complex species and perform a titration simulation to help make an initial guess in setting up the experimental conditions. Literature values for the stability constants need to be input (or guessed based on similar compounds), as well as the pK_a values for the complexant, the self-ionization constant for water and the hydrolysis values for the metal in solution.

Metal hydrolysis occurs as a consequence of the previously explained phenomena that takes place when metal ions in solution surround themselves by water molecules forming the so-called aqua ions. The aqua ions undergo hydrolysis to a major or minor extent depending mostly on the charge to size ratio of the metal ion, and during this process the aqua ions release a proton. Since a proton is released, an associated pK_a value can be determined for this reaction, which can be generically represented by:

$$[M(H_2O)_n]^{m+} + H_2O \rightleftarrows [M(H_2O)_{n-1}(OH)]^{m-1+} + H_3O^+ \qquad (1\text{-}21)$$

The metal hydrolysis is easily explained by considering the inductive effect of the positively charged metal ion. Molecules undergoing inductive effects have an experimentally observable transmission of charge through a chain of atoms, which results in a permanent dipole in a bond. In this case, the positively charged metal ion has an inductive effect that weakens the O-H bond of an attached water molecule, which leads to the liberation of a proton.

In summary, to determine whether the complexant selected for this study could be used for uranium extraction via bioleaching, its acid dissociation constants and binding strength with the metal of interest must be determined. Due to the complexity of working with radioactive materials, the lanthanide, neodymium, will be used as an analog for uranium. In addition, as commented before, polyprotic acids are used as structural and chemical analogs for the siderophore enterobactin during the method development phase. Figure 1-4 shows a flowchart that clarifies the different phases of the process of bioleaching development in a laboratory scale.

The results obtained following this process reveal the ideal pH range for complexation and the strength of complexation relative to other metals. To evaluate the

acid dissociation of the ligands and the subsequent binding constants, different techniques can be applied [37].

1.5 Techniques and methods

Many different techniques have been used to experimentally determine both pK_a values and stability constants in the laboratory [38]. It is recommended, when possible, to determine pK_a values and stability constants from multiple techniques; thus allowing the values to be cross-checked leading to more reliable data. The chosen technique and method of analysis is often dependent on the sample's physical and chemical nature. Many techniques have been used to determine pK_a values and stability constants including: potentiometry [39], spectroscopy [40], conductometry [41], solubility [42], electrophoresis [43], partition [44], NMR [45], polarometry [46], voltammetry [47], kinetics [48], HPLC [49], fluorometry [50], calorimetry [51] and computational techniques [52]. For the present research, three of these techniques were available for pK_a and stability constant determination: ultraviolet-visible spectroscopy, potentiometry and calorimetry. A thorough description of each will follow in the chapters.

For pK_a determination, the general approach involves experimentally measuring a certain parameter's variation as a function of pH, and then plotting this variation against pH to create a sigmoid curve where the pK_a can be determined by locating the inflection point of the curve. For stability constant determination, an analogous methodology is often used, though in contrast, the pH may be fixed while a different parameter is varied. This curve fitting can be done manually using basic Excel or Origin plots, or it can be performed on advanced modeling software such as HySS, HypΔH, HypSpec or Hyperquad [53]. Even

though the techniques used are different, a common method was used for all techniques evaluated in this study: pK_a values and stability constants were determined using titrations. In titrations, the ligand to be characterized is fully dissolved (no precipitation is observed) and placed into a reaction vessel; this solution is called the titrand or vessel solution. Next, a variable specific to the selected technique that correlates to the pK_a or stability constant calculation is progressively measured while a well characterized solution is added in increments of known volume (titrant solution). During this titration process, it is vital to keep the temperature controlled with a thermostatic bath and the ionic strength of the titrand and titrant solutions both need to be adjusted to the same molarity. Depending on the techniques and the chemicals involved, other conditions may have to be controlled as well. For example, an inert environment may be needed during the whole titration if alkali metals and potentiometers are involved.

1.6 Influential factors in technique choice

Since all the pK_a determination methods are very different from each other, it can be difficult to choose. Several factors need to be taken into account in this decision and it is important to keep in mind that if various methods can be used to characterize the same deprotonation reaction, this would be extremely advised. Several factors that influence the choice of method include the available mass of the sample, the solubility of the sample, the samples response to the desired technique, and the chemical structure of the sample. For example, if a polyprotic molecule is being evaluated, then it is important to know how far apart the different pK_a values are. If they are several units of pK_a apart from each other, then they can be determined relatively easily and not as much sensitivity is needed with the

technique. However, if they are overlapping in a range of one pH unit, then the pK_a values may be very challenging to resolve on different sigmoid curves since only one pK_a value is determined per sigmoid curve. This type of sample would need a very sensitive technique with high resolution between close pK_a values.

The solubility of the sample is also a major determining factor. In some cases, the compound is insoluble until a certain pH is reached, as in the case of enterobactin dissolved in pure water. Sometimes, as in enterobactin's case, this can be remediated using a small amount (3% to 5% in volume) of a different solvent such as methanol. Although this would theoretically alter the ionic constant pK_w of the system and therefore the pH calculations, since it is such a small volume of methanol this ionic constant will be considered 14 same as in systems with only water. Nonetheless, the limited solubility and/or need of different solvents creates challenges for some techniques where higher concentrations are needed, such as potentiometry. Other techniques, such as UV-Vis spectroscopy, are simply not suitable to determine the pK_a for every molecule due to intrinsic characteristics of the technique. For example, if the molecule lacks a chromophore to absorb light, then the molecule cannot be characterized by spectroscopy. This is not necessarily the case for determining stability constants by spectroscopy. To determine a stability constant, only the metal or the ligand must absorb light in the concentration range analyzed. If the metal absorbs light, then addition of the complexant will alter this spectra and the shifting of the spectra can be used to determine the strength of the complexation. Taking these many factors into account, Table 1-4 summarizes the pros and cons of each technique. Highlighted are the techniques used in this research.

Knowing all the information stated in this chapter, the focus of this study was

developed: characterizing new pK_a values of enterobactin, confirming the pK_a values that have been reported using other techniques and potentially determining enterobactin's stability constant with neodymium, a trivalent metal which can serve as a chemical analog to the trivalent actinides.

Table 1-1. Uranium mining techniques and their environmental impact

TECHNIQUE	ENVIRONMENTAL CONCERNS
Underground mining	Waste from mining and milling (tailings) that expose groundwater and fauna/flora to heavy metals and radioisotopes
Open-pit mining	Significant erosion and visible fingerprints Waste from mining and milling (tailings) that expose groundwater and fauna/flora to heavy metals and radioisotopes
In-situ leaching	Potential lixiviant excursions Restoration of groundwater conditions

Table 1-2. Bioleaching suitability of the different uranium ores. Adapted from [6]

URANIUM ORE	CHEMICAL COMPOSITION	DEGREE OF BIOLEACHING (+ easy, - hard, +- variable)
Uraninite	UO_2	+
Gummite	$UO_3 \cdot n\ H_2O$	+
Becquerelite	$CaU_6O_{13} \cdot 11\ H_2O$	+
Brannerite	(U, Ca, Ce) (Ti, Fe) O_6	+
Davidite	$(Fe, Ce, U)_2\ (Ti, Fe, V, Cr)_5O_{12}$	+
Coffinite	$U(SiO_4)_{1-x}\ (OH)_{4x}$	-
Uranophane	$Ca\ (UO_2)_2Si_2O_7 \cdot 6\ H_2O$	+-
Sklodowskite	$Mg\ (UO_2)_2Si_2O_7 \cdot 6\ H_2O$	+-
Autunite	$Ca\ (UO_2)_2(PO_4)_2 \cdot 12\ H_2O$	+
Torbernite	$Cu\ (UO_2)_2(PO_4)_2 \cdot 8\ H_2O$	+
Uramphite	$NH_4 \cdot UO_2 \cdot PO_4 \cdot 3\ H_2O$	+
Zeunerite	$Cu\ (UO_2)_2(AsO_4)_2 \cdot 12\ H_2O$	+
Carnotite	$K_2\ (UO_2)_2(VO_4)_2 \cdot 3\ H_2O$	+-
Tyuyamunite	$Ca\ (UO_2)_2(VO_4)_2 \cdot 8\ H_2O$	+-
Zippeite	$(UO_2)_2(SO_4)(OH)_2 \cdot 4\ H_2O$	+
Uranopilite	$(UO_2)_6(SO_4)(OH)_{10} \cdot 12\ H_2O$	+
Johannite	$Cu\ (UO_2)_2(SO_4)_2(OH)_2 \cdot 6\ H_2O$	+
Schroeckingerite	$NaCa_3UO_2SO_4(CO_3)_3F \cdot 10\ H_2O$	+
Urano-organic compounds		+

Table 1-3. Typical microorganisms used bioleaching uranium ores. Modified from [6]

MICROORGANISM	CHARACTERISTIC	pH	T (ºC)
Thiobacillus ferrooxidans	Oxidize Fe^{+2}, S^0, U^{++}, Cu^{+}, Se^{+2}, thiosulphate, tetrathionate, S	1.2-6.0	5-40
Thiobacillus thiooxidans	Oxidize S^0, thiosulphate, tetrathionate	0.5-6.0	10-40
Thiobacillus acidophilus	Oxidize S^0, organic compounds	1.5-6.0	25-30
Leptospirillum ferrooxidans	Oxidize Fe^{+2}, pyrite	1.5-4.5	20-40
Sulfolobus thermosulfiooxidans	Oxidize Fe^{+2}, S^0, S	1.9-3.0	20-60
Sulfolobus acidocardarius	Oxidize Fe^{+2}, S^0	2.0-7.0	55-85
Acidianus brierleyi	Oxidize S^0, yeast extract	1.0-6.0	45-75
Pseudomonas	Accumulate U, Cu, Pb intracellular	7-8.5	4-43
Penicillium	Accumulate U, Ra, Pb in the cell wall	5.0	15-30
Rhizopus	Accumulate U, Th, Ra in the cell wall	4.0-5.0	24-27
Desulfovibrio desulfuricans	Remove U, Cu from the dissolution	4.0-7.0	0-44

Table 1-4. Overview of strong (++) and weak (--) points of pK_a and stability constant determination methods. Modified from [38]

Method	Amount/ Concent.	Restrictions	pK_a range	Cost/time	Precision	T, i.s.
Potentiometry	-	+	-	++	+	+
Conductometry	-	++	-	+	+	-
Voltammetry	-	+	+	+	+	+
Calorimetry	-	++	++	+	+	+
NMR	-	-	++	--	++	-
Electrophoresis	++	+	+	+	++	++
HPLC	++	+	-	+	+	+
Solubility	-	-	+	--	+	-
Spectroscopy	+	+	+	+	++	++

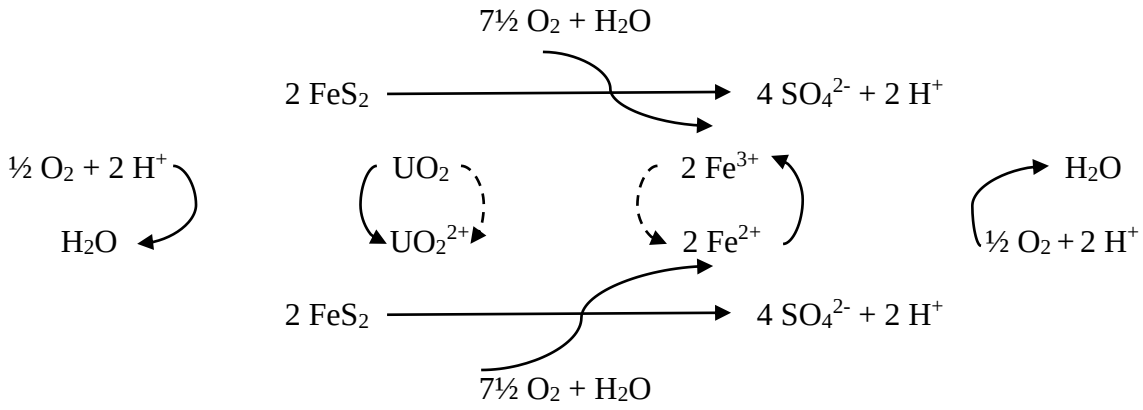

Figure 1-1. Reactions involved in uranium bioleaching. Adapted from [6]

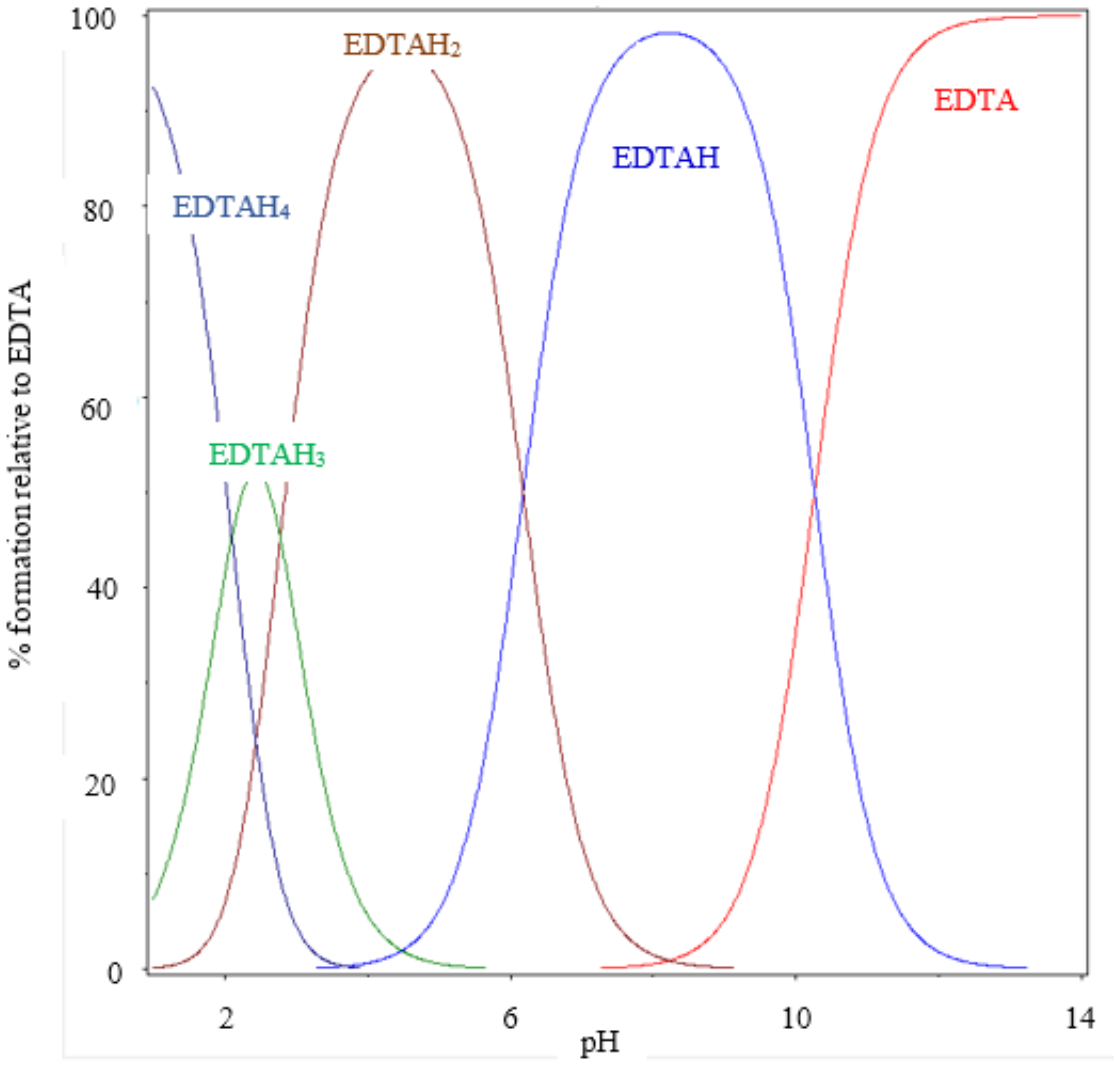

Figure 1-2. Speciation diagram of EDTA produced in HySS

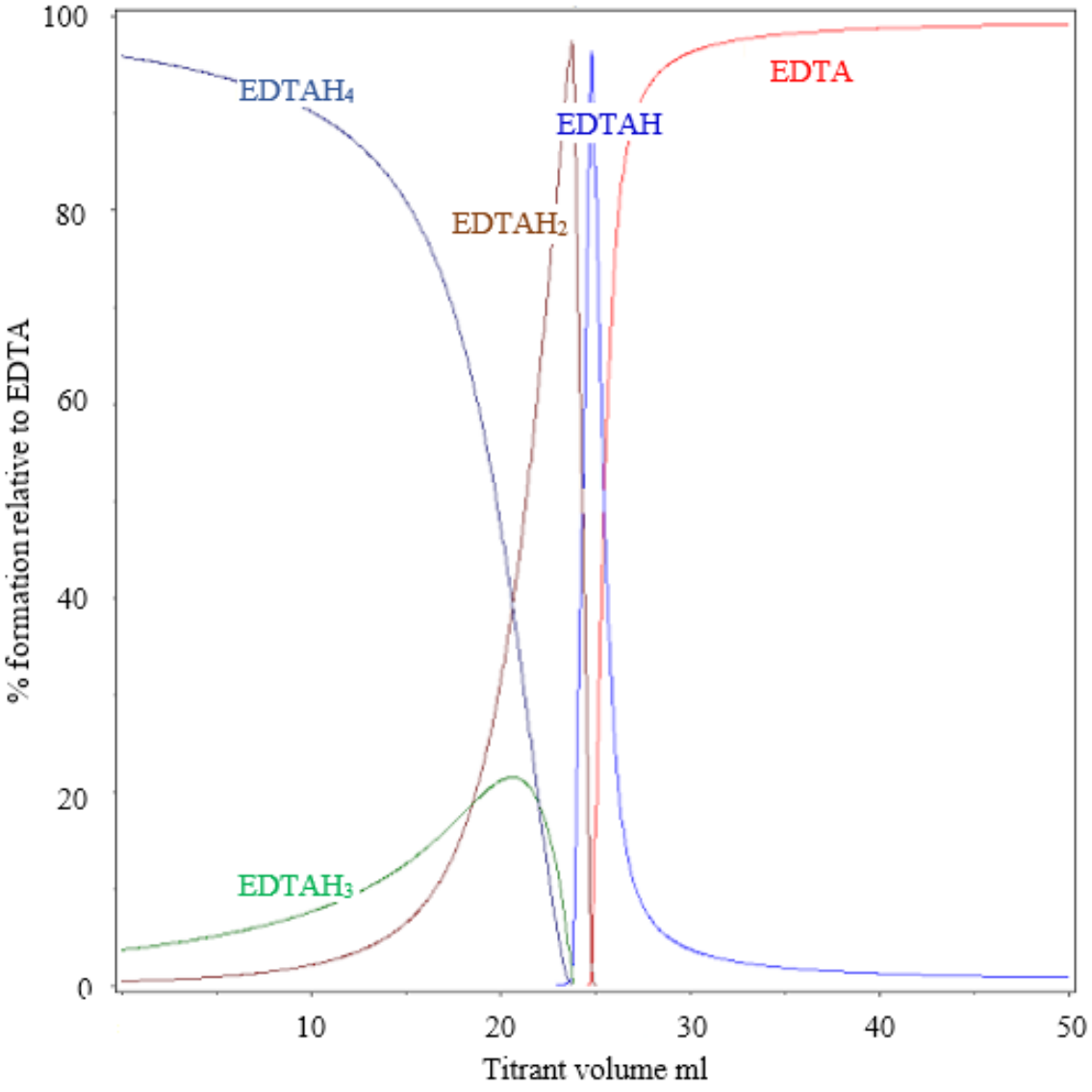

Figure 1-3. Titration simulation of EDTA produced in HySS

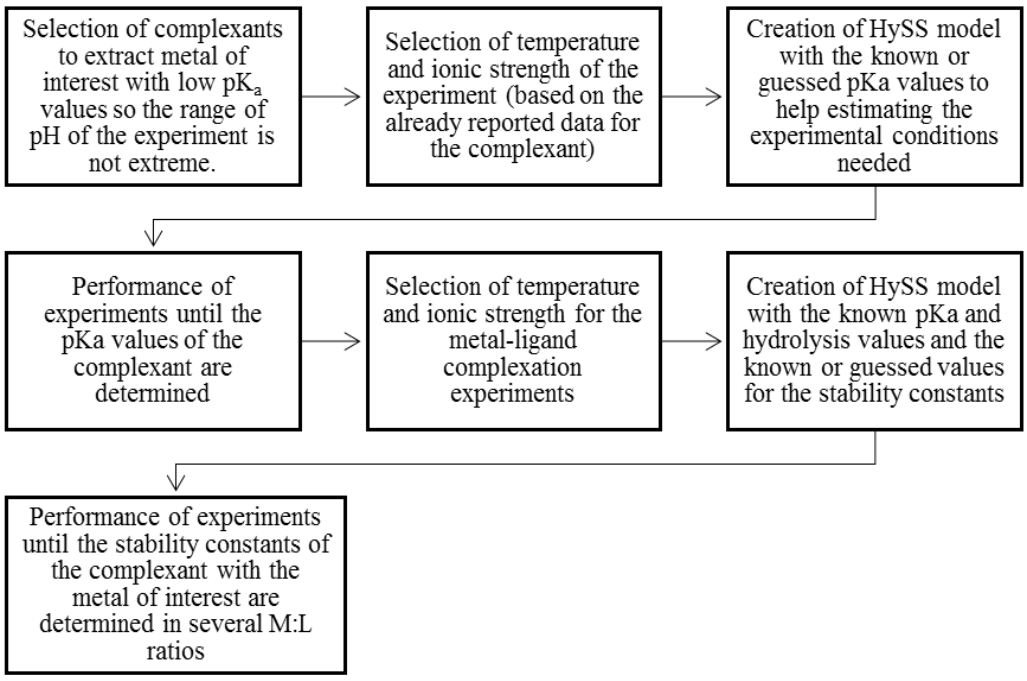

Figure 1-4. Complexation chemistry process for bioleaching trials

CHAPTER 2

POTENTIOMETRY

2.1 Fundamentals of potentiometry

In potentiometry, pH or potential of the titrand solution is progressively measured by an electrode immersed in the solution as the titrant is added. Figure 2-1 illustrates a general schematic of a potentiometric titrator with the various parts identified on the system used for this research, a Metrohm 905 Titrando.

The pH glass electrode is the main element behind the measurement. Generally speaking, for any potentiometric measurement, two electrodes are needed: a reference electrode and an indicator electrode. The indicator electrode provides a potential depending on the composition of the solution being analyzed while the reference electrode supplies a potential that is independent of the sample solution, normally based on standard chemical potentials. The total measured potential of the electrode is the difference between the reference and the sample potential.

Many different electrodes have been used throughout history, the most commonly used ones are glass electrodes. In glass electrodes, the reference electrode and indicator electrode can be built together in a single piece forming what is called a combined electrode. The function and results of a combined electrode are the same as two separate electrodes. A sketch can be seen in Figure 2-2.

Glass electrodes have a glass bulb membrane and an electrically insulating tube, which separates the internal solution (for example KCl) and the silver/silver chloride system from the titrand. The KCl solution has a constant chloride concentration that keeps the Ag/AgCl electrode at a constant potential. The Ag/AgCl electrode is hermetically sealed and connected to the pH meter, which measures the potential difference across the glass membrane. Figure 2-3 shows a schematic of a general glass electrode with the various components identified on the electrode used in this study.

As explained before, all electrodes need two points to measure the potential difference between them; in glass electrodes these points are the electrode contacting the internal solution and the reference electrode contacting the titrand. This potential difference builds up in the outside glass and titrand interface and is measured based on the ion exchange that happens in the glass membrane. Since glass is made of silicon dioxide and doped with oxides of alkali metals, once the glass surface is exposed to water, the silicon dioxide groups start to protonate according to Equation 2-1.

$$Si - O^- + H_3O^+ \rightarrow Si - O - H^+ + H_2O \qquad (2\text{-}1)$$

A scheme of the ionic exchange in the glass electrode can be seen in Figure 2-4. It is of extreme importance that the glass electrodes remain hydrated in order for the electrode to be able to form the hydrated layer displayed in Figure 2-4. If not stored properly, then extensive time and care must be taken to rehydrate the electrode prior to use. The electrode used in this study was consisting stored in 3 M KCl when not in use to maintain this hydration layer. If a different electrolyte is used inside the electrode, such as NaCl, then saturated NaCl should be the storage solution for the electrode. It is also important that the opening slit, which allows the electrolyte solution to be refilled in the electrode, remain

open during the measurements so that the ionic exchange across the glass diaphragm is facilitated. This slit should be closed at the end of the experiments to avoid electrolyte evaporation and precipitation.

The protons start to exchange between the solid glass membrane and the water solution, and since an interface is separating two phases where ionic exchange equilibrium is established, the glass/solution interface starts having a potential difference according to Nernst equation (Equation 2-2).

$$E_{glass\ wall/solution} = \frac{2.303\ RT}{F} \log \gamma_{H_3O^+} \tag{2-2}$$

R is the molar gas constant 8.314 J/(K mol), T is the temperature in K, F is the Faraday constant 96,485.3 C and 2.303 is the conversion between natural and base ten logarithm. $\gamma_{H_3O^+}$ is the activity of hydronium ion, which as explained in Chapter 1, can be considered equal to its concentration under certain conditions.

Equation 2-2 can also be rewritten to account for the offset potentials in the electrode, which can be seen in Figure 2-5. The potentials seen in this figure are analogous in a combined electrode but for a clearer picture two separate electrodes are used in the figure. The offset potentials can be grouped in the variable E', which includes the inside wall/KCl potential (U_2), the reference electrode (U_4) and the indicator electrode (U_3). U_5 is the diffusion potential due to different mobility rates of anions and cations through the diaphragm, and it can be kept constant using suitable reference measures, such as keeping the stirring speed constant during measurements, keeping the diaphragm clean, and using reference electrolytes as concentrated as possible. If U_5 is considered constant, then the changes in the potential of the electrode are simply due to pH changes in the outside solution, represented by U_1 (i.e., the potential of the indicator electrode with respect to the

sample solution).

If the assumption that activity and concentration of the hydronium ions are equal is valid (see Chapter 1 for a full description of this assumption), then the potential of the glass electrode can be expressed linearly as a function of pH, as expressed by Equation 2-3.

$$E_{glass\ electrode} = E' + \frac{2.303\ RT}{F} pH \quad (2\text{-}3)$$

This linear dependence is what allows modern electrodes to display the measurements directly in pH units or in potential units depending on the user's preference. Although because of this reason, special attention needs to be paid to temperature conditions and calibration of the electrode. The relationship between the potential and the pH is directly dependent on temperature, which is why modern electrodes have temperature probes as well, so that an automated electronic temperature correction is done to account for temperature changes.

Although the slope of Equation 2-3 (Nernst slope) is mathematically determined by 2.303RT/F and therefore should only be dependent on temperature and constant for a certain temperature, the interfering ions and the deteriorating processes that the glass electrode may undergo with time can make the actual slope of the electrode not ideal. In order to account for this, different buffers can be used to periodically calibrate the electrode. In this study, NIST approved buffers were used to calibrate the electrode every day before its use. In a potential versus pH curve, the ideal slope in the calibration should be 100%, since the slope represents the current potential divided by the nominal potential. If the experimental calibration was less than 99% or more than 101%, then the buffer solutions were replaced and the calibration was done again. The electrode was also checked in these cases looking for damage signals or partial precipitation or evaporation of the

internal electrolyte in which case new electrolyte solution needed to be prepared.

Glass electrodes have some limitations given by their working principle when used in certain experimental conditions such as high temperature or extreme pH conditions. A common interference is related to alkali metals and it happens when working with very concentrated alkali solutions. The pH displayed is lower than the actual value for the solution because alkali metals (such as Na^+ and K^+) and hydronium ions have similar sizes and the same charge, interfering in the equilibration of the glass/solution interface. Strong alkaline solutions can also damage the glass, as well as fluoride solutions, and solutions with proteins or noble metals can adsorb in the glass.

2.2 Application to pK_a or stability constant determination

Potential is related linearly to pH as shown before in Equation 2-3, and pH is related to deprotonation constant determination through the Henderson-Hasselbach equation, described in Chapter 1 as Equation 1-9. As the potential changes, the pH changes and so does the concentration of protons in solution altering the amount of protons linked to the ligand and therefore the ratio $[A^-]/[AH]$. It is assumed that at very low pH values ($pH < 2$) the ligand will be fully protonated while at very high pH values ($pH > 13$) the ligand will be fully deprotonated. In these cases, it is impossible to determine pK_a values for the ligand simply by plotting the potential versus the volume of titrant added. A sigmoid curve appears giving the potential at equilibrium that corresponds to the inflection point of the curve. Since potential and pH follow a linear relationship, it would also be possible to plot pH versus volume of titrant and then the inflection point of the curve would correspond to the pK_a value. If the ligand happens to have several pK_a values there would be a sigmoid

curve for each one of them. In the case of stability constant determination, as the pH of the vessel solution varies, the protonation of the ligand varies, and the more deprotonated the ligand, the more potential binding sites that become available for the metal. Therefore, as the pH of the titrand varies, so does the amount of complex formed, and a similar curve, as in pK_a determination, can be plotted for stability constants.

If the chemical system analyzed by potentiometric titrations is very complex, then it can be challenging to determining the inflection point of the sigmoid curves using basic Excel plots. Alternatively, experimental data from potentiometric titrations may be determined using HyperQuad. With the pH or potential measurements and the initial concentration and pH values of the solutions in the burette and vessel, a very accurate calculation of the concentrations of complex and free metal and ligand and potential protonated species can be obtained with titration time. From this information, stability constants can be determined following Equation 1-15 from Chapter 1. After developing a model for the chemical system in HySS (as described in Chapter 1), HyperQuad then takes the experimental data and refines it to adjust it to the theoretical HySS model in the best way possible.

2.3 Procedure and experimental considerations

As mentioned before, many different techniques may be used to determine pK_a and stability constants, but only one method was used in these studies, titrations. In potentiometry, the titrand containing the ligand is adjusted to a certain pH value and ionic strength then placed in a suitable vessel, and the temperature probe and combined glass electrode are immersed in the solution. A burette with a dosimeter is loaded with the titrant

that is adjusted to a certain pH and the same ionic strength as the titrand. The tip of the burette is then placed in the vessel with the titrand just above the level of the solution. If not kept above the level of the solution, then the titrand will diffuse in the burette tip and both titrand and titrant will be delivered in each injection instead of just titrant altering the actual volume of titrant added to the vessel. As an alternative, a Metrohm prebuilt anti-diffusion tip can also be used if the burette tip needs to be submerged in the titrand. As the titrant is added, stirring is performed with a magnetic stir bar and the pH is measured after each injection from the burette. Jacketed vessels can be connected to a temperature controlled bath and a Teflon lid can be used if an inert environment is needed.

Since the titrator is fully automated, after both solutions have been prepared and placed in suitable containers, the titration can be controlled using a computer and the Tiamo software. In this research, Tiamo 2.4 was used. Each of the components of the titrator can be controlled using Tiamo: the temperature probe measurements, the pH or potential measurements, the volume delivered by the dosimeter and the stirring bar speed. It is also possible to take independent pH measurements in a solution using the manual control of Tiamo without needing to perform an experiment.

Once the electrode has been calibrated with NIST standards, the dosimeter needs to be prepared using Tiamo's manual control. Next, the electrode, temperature probe and burette tip can be placed for the titration vessel. If needed, then the temperature can be regulated by the jacketed bath and an inert atmosphere can be created with nitrogen. Once the experimental setup is complete, the titration can be programmed in Tiamo. A new method can be created or one of the templates in the system can be used. Tiamo allows several methods of titrations to be completed. In addition, the pH or potential can be

measured. The titrant may be added in increments of the same volume (MET command) or the volume injected may be varied according to the proximity to an endpoint (DET command). Far from an endpoint, larger volumes of titrant are added and near an endpoint, small volumes are injected. The stirring rate and the stopping parameters may also be varied (i.e., stop at a certain volume, stop after finding a certain amount of end points or others). Other parameters can also be adjusted in order to refine the titration method depending on the chemicals used.

2.4 Data produced and how they helped in the method development process

In order to make the method development process more cost effective, enterobactin was replaced with polyprotic acids in this phase of the study. EDTA, HIBA and citric acid were used as ligands in this phase because their chemical structure and complexation behavior is similar to enterobactin. During the experiments with EDTA and HIBA no temperature bath or inert environment conditions were applied (i.e., the titrand vessel was open to the laboratory environment). This implies potential carbonation issues and temperature fluctuations that could lead to inconsistent measurements. Both carbonation and temperature fluctuations were actual issues in our laboratory and they will be further explained later on in this chapter.

Initially, EDTA was used to determine an experimental protocol that could be used for enterobactin, but the limited solubility of EDTA made it challenging to use. Hence, HIBA was then evaluated because of its increased solubility in solution. However, since EDTA has a much greater chemical resemblance to enterobactin, more effort was put into

developing a method with this molecule. These efforts implied working in a limited range of pH for facilitating solubility of EDTA, preparing individual solutions of EDTA for each of the experiments instead of diluting from a stock EDTA solution and other considerations.

Titrations to find the pK_a values from EDTA were performed with both NaOH and HCl as titrants. Different titrations were simulated until the most suitable conditions were found using the reported values in the IUPAC Stability Constant Database [54] as a theoretical reference in the HySS model. This database contains all significant published stability constants with full literature references and additional information, containing data from 1887 up to date. Figure 2-6 shows two titrations from acid to base and from base to acid, respectively. Ionic strength of the vessel and burette were adjusted to 0.1 M using NaCl. The reaction vessel contained 0.001 M EDTA and the pH was adjusted to 1.7 and to pH 13.0 using HCl or NaOH, respectively. If an acidic pH was used in the reaction vessel, then the burette would contain 0.05 M NaOH; while if a basic pH was used in the reaction vessel, then 0.1 M HCl was used in the burette.

The results from these initial experiments were very challenging to reproduce. Stock solutions of titrand and titrant were made in order to perform this same experiment two or three times and each of the experiments resulted in a different number of end points. This was initially attributed to the possible fluctuations in the room temperature or experimental inaccuracies when preparing the stock solutions.

Since results closer to the theoretical reported values were found titrating from acid to base, the first titration was tried again recalculating the exact concentrations of the chemicals actually measured. Figure 2-7 shows the plot obtained by the titration of 0.001

M EDTA containing HCl to adjust the pH in the reaction vessel to 1.8. This solution was then titrated with 0.501 M NaOH to pH 12.7. Both solutions were adjusted to 0.1 M ionic strength using NaCl and the temperature recorded by the potentiometer was roughly 24.5 ^{o}C.

Database values of EDTA only report two of these end points as pK_a values, 6.19 and 9.86, which would roughly correspond to EP3 and EP6 in this titration. EP4 is most definitely due to the HCl-NaOH neutralization reaction and EP1, EP2 and EP5 are likely due to carbonation interferences.

These data were input in HyperQuad and compared to the theoretical model, after previous adjustment of the model to the exact concentration and volumes from the experiment. Figure 2-8 shows the HyperQuad data treatment, where the red line is the theoretical model and the blue diamond line is the experimental data. Since only one titration was performed for checking the validity of the method, uncertainty analysis for this data set is not available.

The data did not converge in HyperQuad, meaning the program could not refine the pK_a values to adjust the experimental data to the theoretical model, or if it could, then the values were refining further away from the initially input theoretical values. Further investigation was done to find out possible causes for this to happen. Some factors in HyperQuad needed to be actualized to match our system such as:

a) Burette error: five aliquots of 4 ml ultrapure water were weighed and their temperature was measured. The volume was then recalculated using the density of water at that temperature obtaining a mean of 3.99315 ml and a standard deviation of 0.00518 ml. This information was input in HyperQuad actualizing

the default calibration factor on the .ini file as 0.998288.

b) Titre error: this parameter was actualized from default to the standard deviation obtained with the five aliquots experiment: 0.00518 ml.

c) Electrode error: was actualized using the calibration performed that day up to 0.001 pH units.

Even with these factors actualized, the data still did not converge, which lead to the conclusion that temperature control and carbonation may be the main reason why the data were not converging. A jacketed cell was used from this point on, and connected to a water thermostat bath kept at 25 ºC. Regarding carbonation, a more labor intensive process needed to be performed to eliminate the problem. Carbonation is the phenomena by which carbon dioxide from the environment is absorbed by alkali solutions according to the following equation:

$$OH^- + CO_2 \rightarrow HCO_3^- \quad (2\text{-}4)$$

This may not have an evident effect in the concentration change but at the end point, some alkali is going to be consumed in the reaction:

$$HCO_3^- + OH^- \rightarrow CO_3^{-2} + H_2O \quad (2\text{-}5)$$

While this should be employed in the ligand deprotonation reaction, the immediate effect of carbonate contamination is that the pH is higher than it should be, and therefore when a stability constant or a pK_a value is being determined using a carbonated solution, the carbonate impurity will introduce an error in the pK_a or stability constant value.

As this seems to be a common problem, our system was tested to see which degree of carbonation was present. More than 2% carbonation contamination is unacceptable in most published data. To evaluate the impurity in the HCl and the NaOH, a strong acid-

strong base titration was performed. The potential was measured as a titration was performed according to the method GLEE, which was described in the HySS software for carbonate contamination [55]. The results are shown in Figure 2-9. The protolytic impurity level, also known as carbonation level, is almost 11%, much higher than the acceptable value. GLEE adjusts the data to the Gran function [56] producing a plot as shown in the figure, which can also be used to calibrate the electrode as an alternative to the standardized buffer method. Three different points are distinguished in this function. At the equivalence point Gran function equals 0, before the equivalence point Gran function equals ϕ and after the equivalence point Gran function equals ϕ'.

$$\phi = (V_{titrant} + V_{titrand}) \cdot 10^{-pH} \quad (2\text{-}6)$$

$$\phi' = (V_{titrant} + V_{titrand}) \cdot 10^{pH} \quad (2\text{-}7)$$

In order to reduce carbonation to acceptable levels, it is necessary to take special care of alkali solutions before and during titration experiments using a rigorous alkali solution preparation and performing the experiment under an inert environment. For the preparation of alkali solutions, it is necessary to boil the milli-Q water used for the solutions under a nitrogen environment so that the water is CO_2-free. For this purpose milli-Q water was boiled and distilled in an experimental setup as shown in Figure 2-10 under a nitrogen environment.

This water should be stored under a nitrogen environment and the alkali solution should be prepared using this water in a nitrogen environment as well. An inert glove box was used to store the solutions used in this work. Also, all alkali solutions should be stored in plastic instead of glass containers because glass contains silicates that produce a similar effect as carbonate ions.

To ensure that no carbonate was introduced during the potentiometric titration, the whole titration vessel should be sealed and nitrogen should be flushed through the system as the experiment is performed. If possible, as in the case of the titrator used in this research, a tube filled with soda-lime should be attached to the dosimeter, also reducing the amount of carbonation that can be introduced to the titrant.

To make sure carbonation has been reduced, it is recommended that a Gran's plot is performed again using a standardized acid to titrate a standardized base and the GLEE software to check the levels of impurity. To standardize the acid and the base, primary standards should be used, such as borax with methyl red as an indicator for the acid and potassium hydrogen phthalate with phenolphthalein for the base [57]. Borax was used without further purification from a commercial source, while potassium hydrogen phthalate was dried by heating to 120°C for at least 2 hours and stored in a covered vessel inside a desiccator.

For this Gran's plot test, a 0.1 N NaOH solution was prepared inside the glove box by dissolving 50g of NaOH in 50 ml of water, equilibrating it and allowing the solid to settle. The supernatent solution yielded a 0.1 N solution when 6.5 ml of it was diluted to 1 liter. A solution of 0.1 M HCl was prepared from commercial concentrated HCl.

Once the solutions were prepared, sufficient amount of the appropriate primary standard was measured to give an endpoint well in excess of the burette accuracy. This was placed in the titration vessel and dissolved in roughly 25 mL of distilled, CO_2-free water, adding one drop of the appropriate indicator. HCl and NaOH were titrated to the first permanent color change (to pink for both indicators). The concentration of the solution was then back-calculated precisely. This was done five times or until the concentration of the

solution was known within a 2% error.

With the exact concentrations of the acid and base known, an HCl-NaOH titration was performed in the potentiometric titrator and the data were input in GLEE producing a Gran plot and giving a new value for the amount of carbonation in the samples. Figure 2-11 shows the new carbonation impurity level.

As can be seen, the procedure followed above significantly helped reduce the amount of carbonation interfering in the potentiometric titration down to less than 1% impurity.

Once this was done, a new experiment was performed to try to test our potentiometric method. A new polyprotic ligand was tried because of its affinity to enterobactin was similar to EDTA but it was easier to work with: citric acid. The experiment and data of a recently published research paper were recreated in our laboratory [58].

Because in this experiment the use of perchloric acid and perchlorates is needed, our electrode needed to be filled with saturated NaCl and stored in this solution as well, since if KCl was used $KClO_4$ could have been formed. It was then calibrated with standardized NIST buffers as before. The temperature bath was kept at 25 ºC with the thermostat bath, nitrogen was flushed through the system during the experiment and 10 minutes of mixing were allowed between injections.

The titrant consisted of 50 ml of 0.2088 M NaOH and sodium perchlorate to adjust the solution to 1 M ionic strength. Titrand consisted of 80 ml of 0.0134 M neodymium nitrate and 0.055 M citric acid plus sodium perchlorate to adjust the solution to 1 M ionic strength.

The experimental data were collected using the Tiamo software and compared to a HySS model that was built according to the constants from literature and the initial estimate on the complexes stability constants was done according to the data reported [58]. HyperQuad was used to do this comparison and Figure 2-12 shows the data plotted exactly as in the software.

As can be seen in the plot, the experimental values (blue diamond points) and the model created in HySS (red dotted plot) resulted in very good agreement and HyperQuad was able to refine the experimental data to adjust it to the theoretical model and produce stability constants specific for our experiment. Table 2-1 shows a comparison between the refined constants for our experiment and the reported constants in [58].

As can be seen, there is still some disagreement between the reported constants and the obtained constants in this laboratory. NdCit stability constant disagrees by 8.6%, NdCitH by 4%, $NdCit_2$ by 8.1% and $NdCit_2H$ by 5.8 %. Even though none of these constants disagrees in more than 10% within the reported value, some sources of error could be the main cause. The reported constants are calculated at 1.06 M ionic strength while the experimental ones are determined at 1 M ionic strength. Also, the reported constants were determined with standardized solutions. In the experiment, this standardization was not performed since this process is time consuming and strenuous and the data were only used to check our methodology. For the same reason, our experiment was only performed once, therefore the standard deviation shown in the experimental constants corresponds to the HyperQuad refinement, while the reported standard deviation corresponds to an analysis of three replicate experiments.

Once the potentiometric method was proven successful with already reported data

in the method development process, its role in stability constant and pK_a value determination for enterobactin was considered. Further discussion about this will follow in Chapter 5, which focuses on enterobactin experiments.

Table 2-1. Comparison of reported and experimental constants refined with HyperQuad

Species	Stability constant, β	
	Reported value [58]	Refined experimental values
NdCit	6.94 ±0.03	7.5875 ±0.0170
NdCitH	9.5±0.2	9.9920 ±0.0247
$NdCit_2$	10.91 ±0.01	11.8679 ±0.0193
$NdCit_2H$	14.5 ±0.2	15.3902 ±0.0278

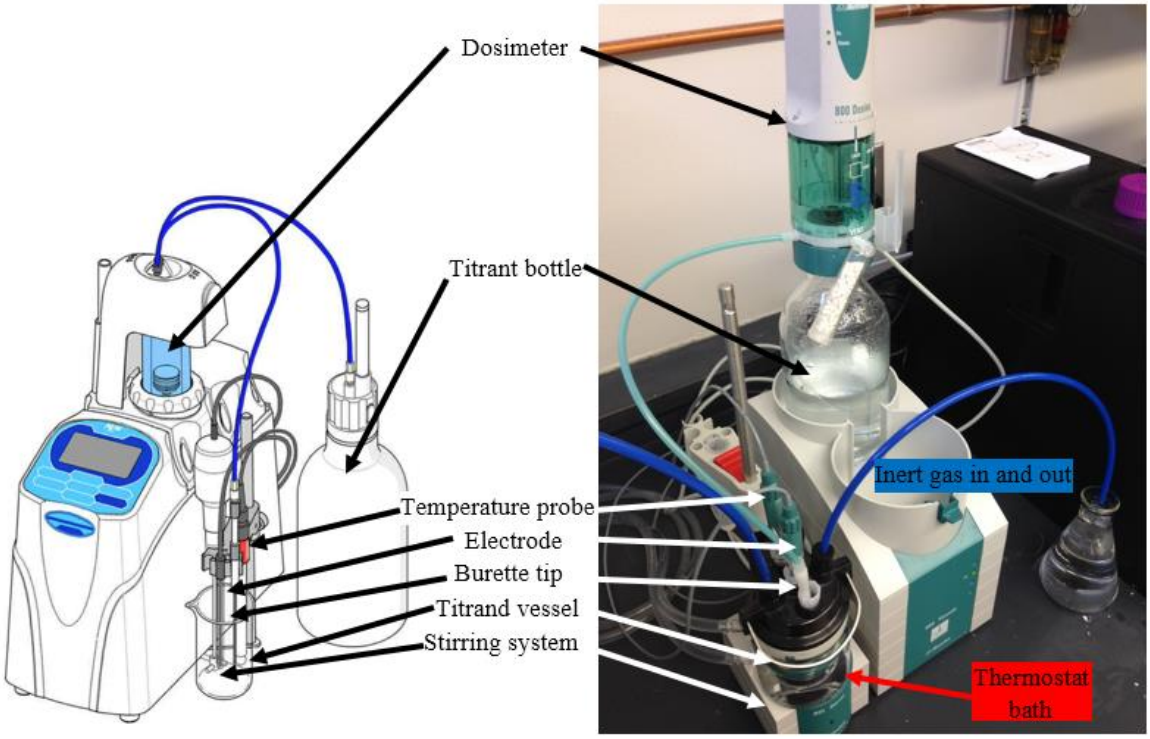

Figure 2-1. Potentiometric titrator. Modified from Scientific Gear AT-700 website

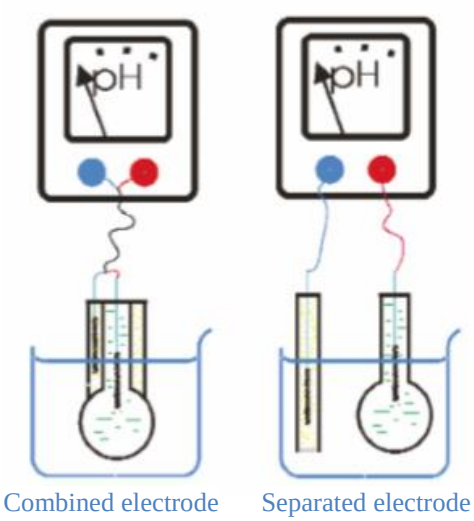

Figure 2-2. Combined and separated glass electrodes. Modified from [59]

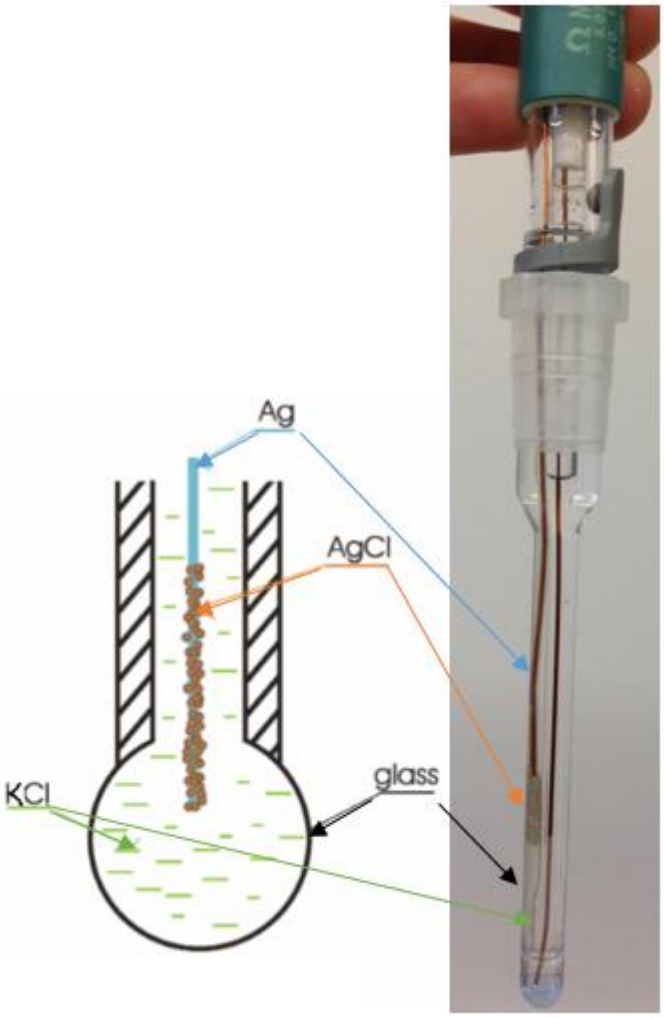

Figure 2-3. Glass electrode. Modified from [59]

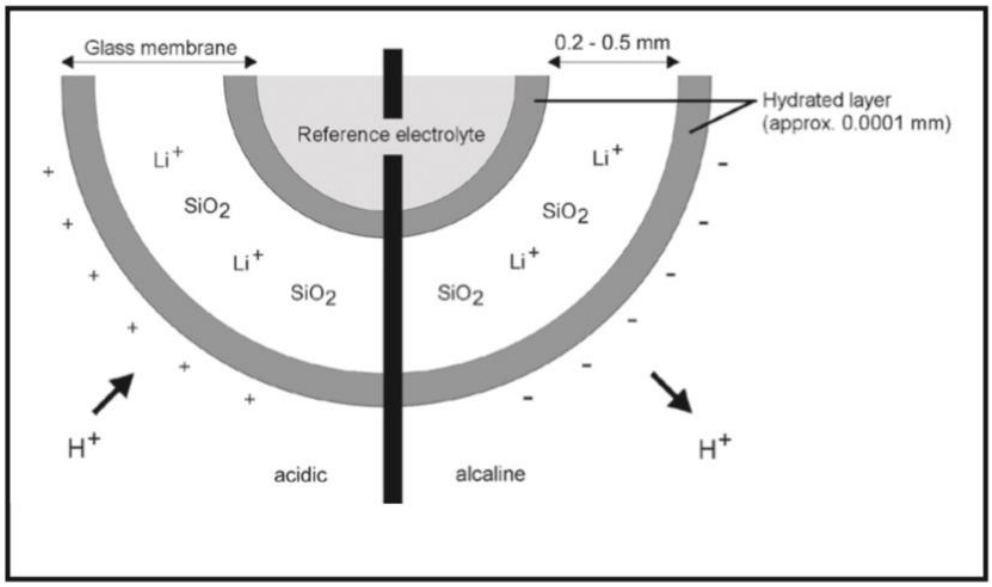

Figure 2-4. Ionic exchange in glass electrode. Modified from [60]

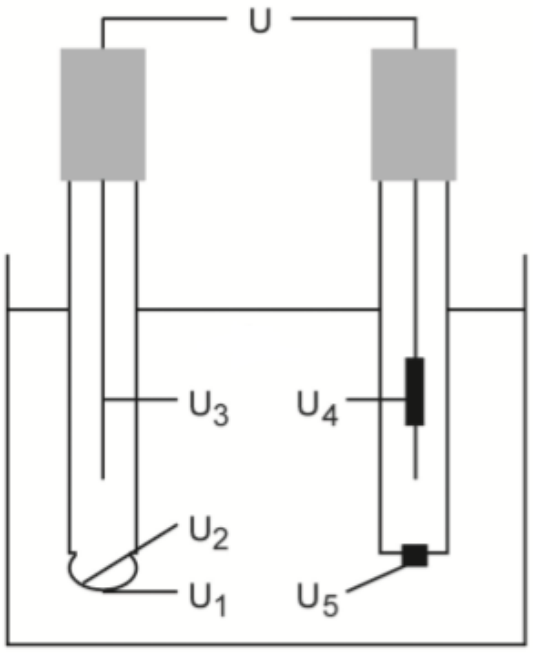

Figure 2-5. Sites of potential in a glass electrode system. Modified from [60]

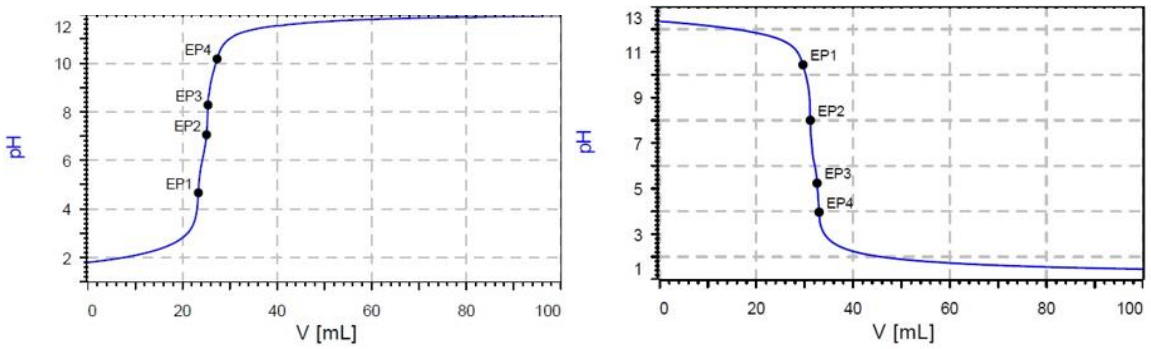

A B

Figure 2-6. Titration of EDTA with NaOH (A) and HCl (B)

End points

DET pH	DET pH.1				
EP1	3.769	pH	13.4664	mL	
EP2	4.940	pH	13.8980	mL	
EP3	6.206	pH	14.4126	mL	
EP4	6.918	pH	14.7919	mL	
EP5	8.686	pH	15.1838	mL	
EP6	9.541	pH	15.7638	mL	

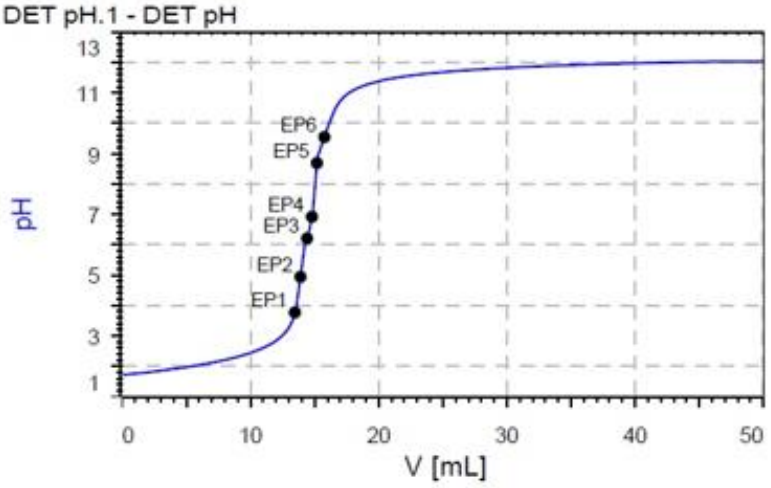

Figure 2-7. Titration of EDTA with NaOH

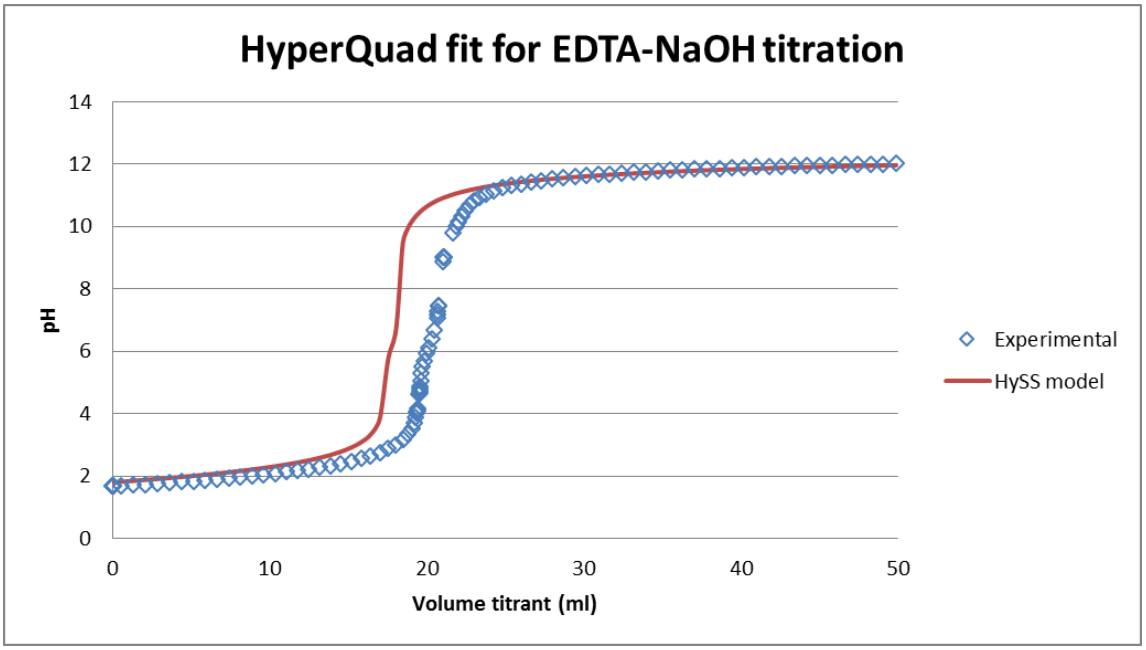

Figure 2-8. HyperQuad data processing of the EDTA-NaOH titration

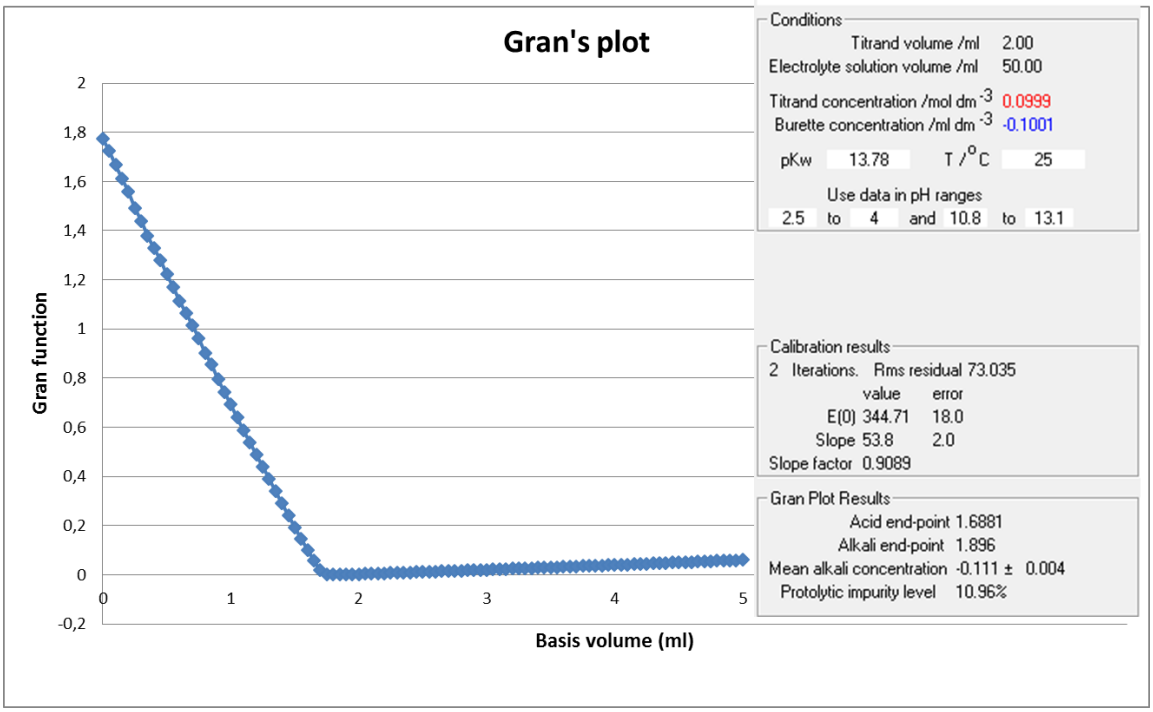

Figure 2-9. GLEE results for carbonation test

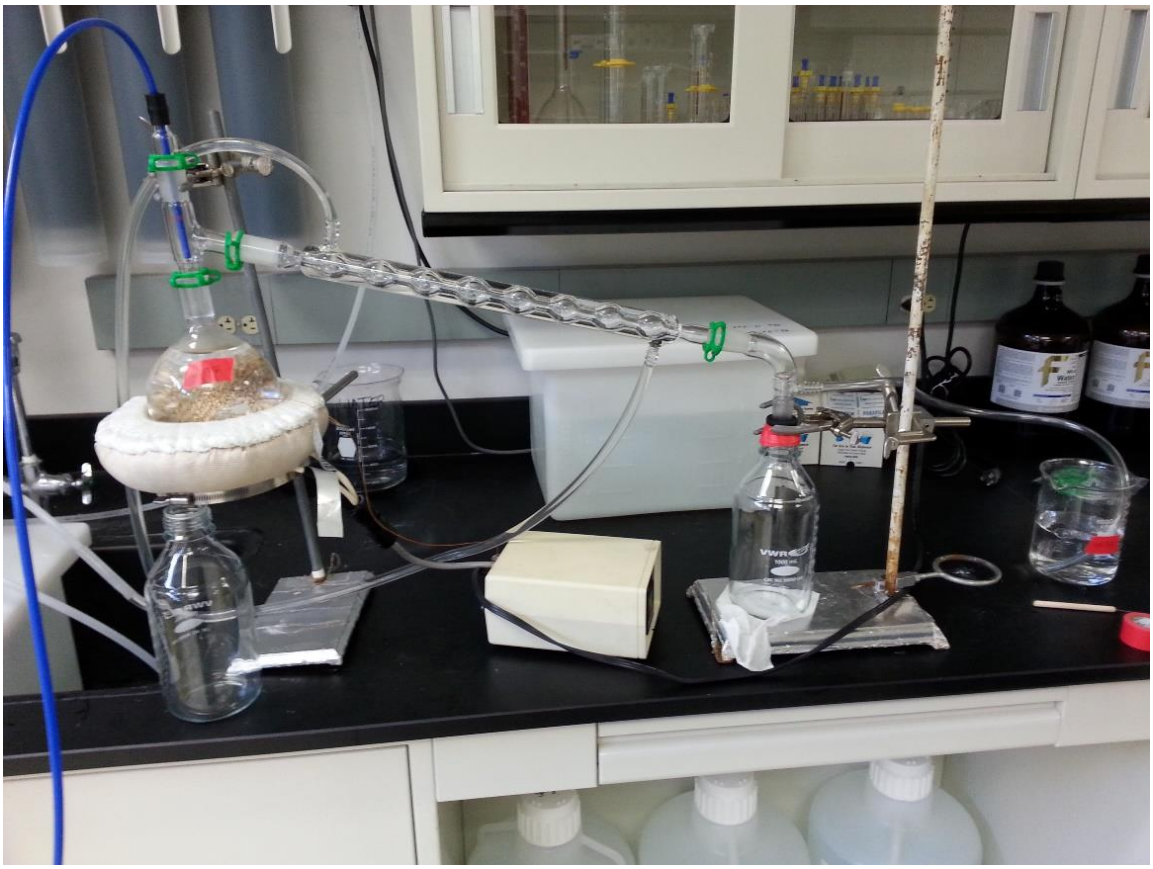

Figure 2-10. Setup for distillation of CO_2-free milli-Q water

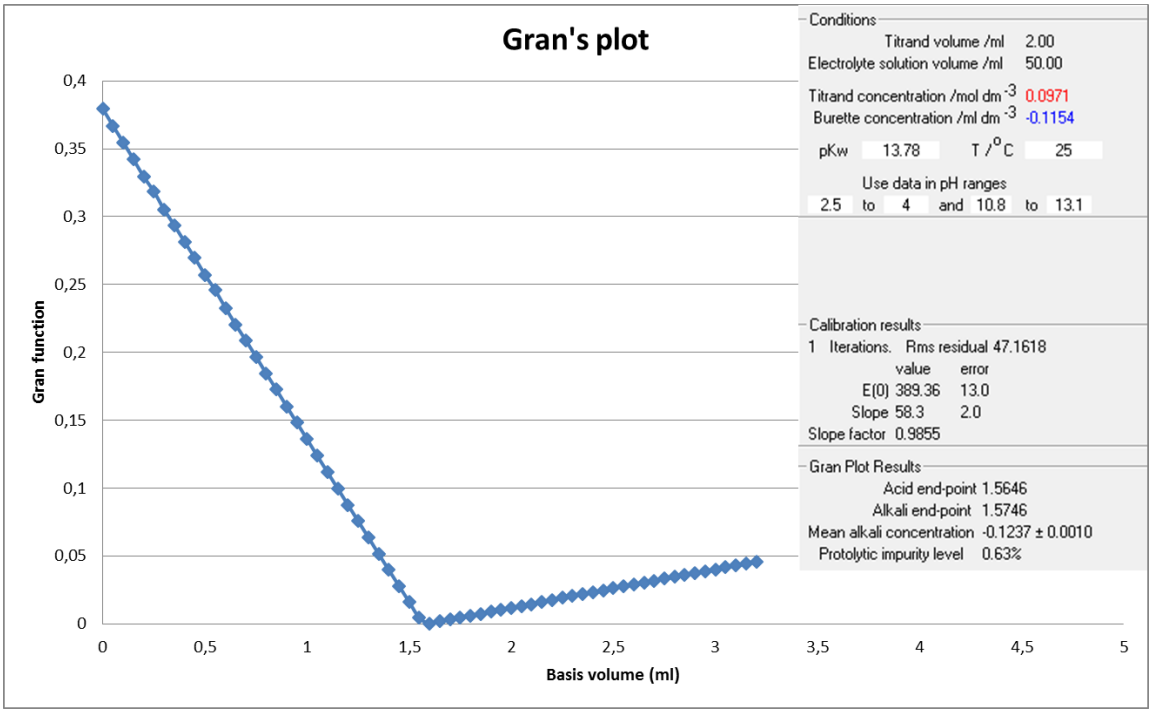

Figure 2-11. GLEE results with carbonation removed

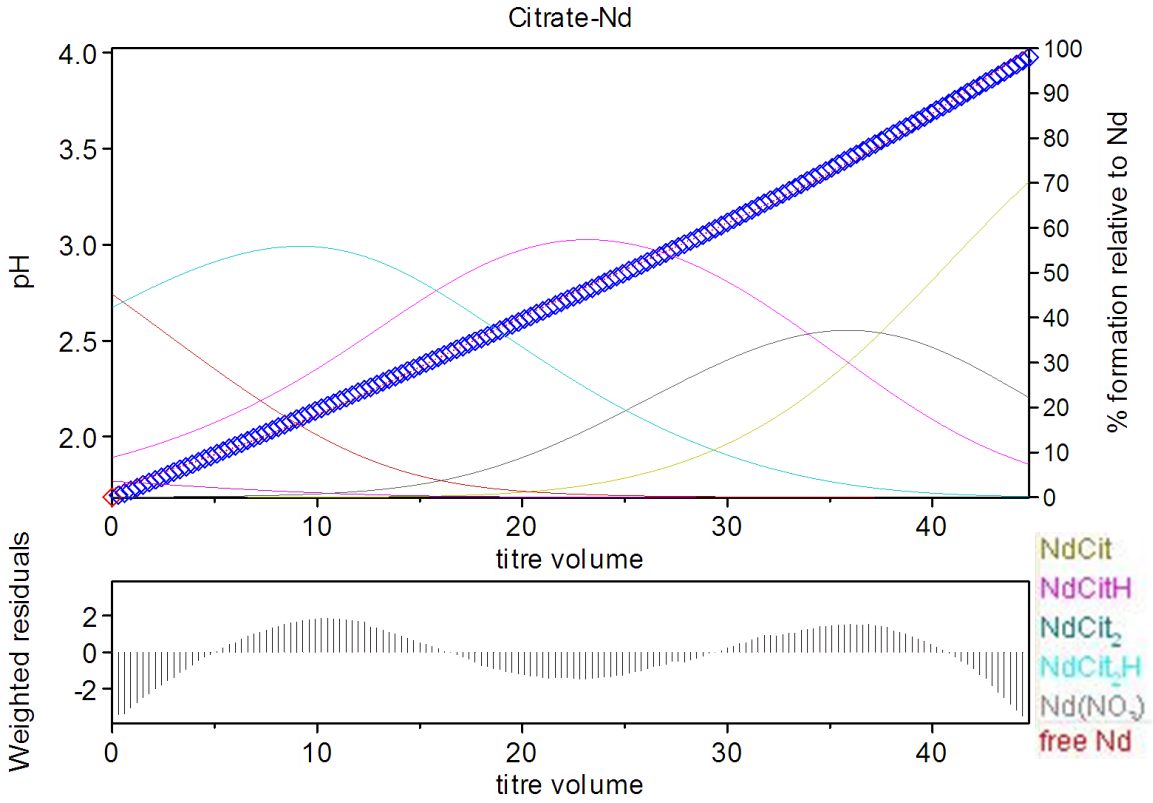

Figure 2-12**.** HyperQuad results for neodymium-citrate complexation

CHAPTER 3

UV-VIS SPECTROPHOTOMETRY

3.1 Fundamentals of spectrophotometry

Spectrophotometry is the measurement of the absorbance of a solution. Absorbance is the measure of the capacity that a substance has to absorb light at a specific wavelength of the electromagnetic spectrum, in particular in the UltraViolet (UV) and visible range (190nm-380nm and 380nm-750nm). Therefore, UV-Vis spectrophotometry only works with substances that are sensitive to UV-Vis light. When photons from the UV-Vis light interact with the molecule, electrons become excited, absorbing energy as they transition from ground state to an excited state [61]. These electronic transitions are possible only in molecules containing nonbonding or π-electrons, since when they absorb UV or visible light they get excited to a higher molecular orbital [62]. Nonbonding electrons are electrons not engaged in a covalent bond and π-electrons are electrons in π-bonds; delocalized covalent bonds are created in some molecules when not enough electrons are present to allow the formation of double bonds and the unbound electrons are then shared around the molecule strengthening all of the bonds equally.

A diagram with the parts of a UV-Vis spectrophotometer resembling the one used in this study (Cary 300 from Agilent) is shown in Figure 3-1. Most of the parts of this instrument can only be seen while disassembled due to its commercial configuration.

Many different instrument configurations exist, though in general, it is best to choose a double beam configuration when working with solutions with multiple species to simplify the process of obtaining a representative absorbance value for the species of interest.

To produce both UV and Vis light both deuterium and tungsten-halogen lamps are used [63]. The deuterium lamp produces ultraviolet light and the tungsten-halogen lamp produces visible light. This light then goes through a filter and premonochromator that increases the working range of the spectrophotometer up to five absorbance units. Next, the light passes through a Czerny-Turner monochromator [64], which accounts for multiple parts: the entrance slit, the collimating mirror, the diffraction grating, a second collimating mirror, and the exit slit. If a double beam spectrophotometer is used, then the light exiting the monochromator goes through a beam splitter and passes through both the reference and the sample cell. The sample cell contains the analyte to be characterized and the reference cell contains the exact same solution minus the analyte. The instrument software compares the spectrum from the sample and the reference cell and subtracts the sample from the reference displaying a final spectrum that corresponds only to the analyte of interest.

Signal is detected in a spectrophotometer using a PhotoMultiplier Tube (PMT) [65]. In the PMT, an incoming photon hits a thin metal film maintained at a large negative potential placed inside of a vacuum tube. The metal film emits electrons as a consequence of the photon hit and these collide with a series of electrodes in the vacuum tube (dynodes) maintained at progressively lower potentials. Each dynode emits several electrons in response to each incoming electron, resulting in a large amplification of the signal. Proper functioning of a PMT requires a constant voltage across the PMT, and PMTs are also

wavelength dependent. This dependence relies on the metal used for the thin film and most PMTs exhibit the greatest sensitivity around 400 nm. For the Cary 300 used in this study, the PMT uses a multialkali metal film.

The only photons that hit the PMT are those that were not absorbed by the sample. The measured absorbance can be correlated back to the concentration of the sample in solution using the Beer-Lambert law [66].

$$A = log_{10}\frac{I_0}{I} = \epsilon cL \tag{3-1}$$

In this law, A is the absorbance, I_0 is the intensity of the incident light at a given wavelength, I is the transmitted intensity across the cuvette, c is the concentration of the species in solution, and L is the path length (cell length). Finally, ϵ is the molar absorptivity coefficient, which is a molecular property constant in a given solvent, at a certain temperature and pressure, with units of $(M \cdot cm)^{-1}$. In most experiments, sample's molar absorptivity and the path length are constant. Hence, measuring the absorbance can yield the concentration of the analyte in solution. Furthermore, it is important to note that the longer the cell path length, the greater the sensitivity of the measurement.

3.2 Application to pK_a or stability constant determination

In order to determine pK_a values using spectrophotometry, the molecule of unknown pK_a values needs to have a chromophore (part of the molecule responsible for its color) close to the ionization site so that the spectra produced by it varies depending on the different dissociation stages. The spectra will change in all wavelengths apart from the ones corresponding to isosbestic points (points where both the protonated and deprotonated sites of the molecule have the same absorbance value) but the difference in absorbance will be

more or less pronounced depending on the wavelength. If the absorbance of the molecule at different wavelengths is plotted against pH, then a sigmoid curve can be obtained and the pK_a values can be determined by the inflection point of the curve [67]. As in potentiometry, this can be done using simple calculations in Excel plots or it can be done using HySS modelling and the HypSpec software package to adjust the experimental data to the theoretical model.

UV-Vis spectrophotometry can also be used to determine stability constants if either the metal or the ligand are sensitive to one of these types of light. As the complex forms, a shift in the spectra will happen and an isosbestic point will be observed progressively. These data can then be analyzed in a similar way as in the pK_a determination case.

3.3 Procedure and experimental considerations

As mentioned before, pK_a and stability constants are determined through titrations. The titrand in the sample cells and the content of the reference cells are placed in a quartz cuvette, which is generally 1 cm long along with a small stirring bar to improve sample mixing during the titration. In these experiments, a multicell holder was used to regulate the samples and references at a constant temperature. The temperature inside the cell holder is measured with a thermocouple connected to the temperature bath. The temperature regulated multicell holder could only be used for 1 cm samples cells. It was possible to make measurements using longer sample cuvettes (up to 100 cm); however, temperature regulation and stirring where not available for these larger cells in the instrument used in this study.

The sample and reference cell are then enclosed in the instrument to reduce noise from background light. The spectra of the sample cells can be recorded using the Cary 300 software. In this software, the 'Scan' function can be used to record the absorbance of the sample over a certain range of wavelengths. For this purpose, the wavelength range is selected, along with some other parameters that control the speed at which the spectra will be recorded and the precision of this measurement. Also, the principle used for measuring the cells content should be selected. For this study, 'Double,' was selected in order to subtract the sample and reference spectra displaying only the difference between them.

After the titrand spectrum has been measured, different injections of titrant are performed manually using a pipette. After each injection, the spectra can be recorded to observe possible isosbestic points that indicate a pK_a or stability constant. It is important to note that the pH and ionic strength of the titrant also need to be adjusted before the injections are made.

3.4 Data produced and how they helped in the method development process

Before any other experiments were done, two parameters needed to be characterized in the UV-Vis spectrophotometer: the concentration range that the instrument was able to detect, and the liquid height (in other words, the volume of liquid in the cell) needed to obtain a consistent spectrum.

With the purpose of estimating the concentration limit that the instrument could detect, a solution containing a species of known UV-Vis spectra was used, in this case, neodymium nitrate. This substance was chosen for its easily recognizable absorbance

spectrum, and its ability to serve as a chemical analog to the trivalent actinides. Solutions with different neodymium concentrations ranging from 0.001 M to 0.5 M were prepared and the spectra for each of them was recorded, as can be seen in Figure 3-2.

The observed neodymium spectra match previously published literature [68]. From the range of neodymium's concentrations measured, a calibration curve was developed to calculate in the detection limit of neodymium, as seen in Figure 3-3.

Since the slit height of the instrument (the height at which the light hits the cell) cannot be modified in the Cary 300, it was necessary to perform an experiment that would determine the minimum volume of sample needed in the 1 cm cuvette to record a consistent UV-Vis spectra. In this liquid height experiment, a solution containing a 0.05 M neodymium nitrate solution was placed in a 1 cm sample cell and the spectra was recorded. Then, 0.08 ml of the same solution was injected into the cell and the spectra was recorded again, until reaching a volume for which the spectra would be consistent. The concentration of neodymium nitrate was chosen to fall within the concentration range determined in the previous experiments, in order to make sure that the signal would be observable by the instrument. Figure 3-4 shows the corresponding spectra for the different liquid heights.

As can be seen, the spectra varies significantly until a volume of 2.21 ml is reached. Therefore, it can be said that a minimum volume of 2.21 ml is needed in the cuvette for obtaining a consistent spectra in the spectrophotometer.

Once these two parameters were determined, experiments were performed with polyprotic acids and neodymium to develop an experimental procedure that could be used to study enterobactin. Initial studies used EDTA, HIBA and citric acid.

Since EDTA is more challenging to use due to its limited solubility, initial

experiments utilized HIBA. Both the sample and the reference cell contained NaCl to adjust the ionic strength to 0.1 M. The pH was adjusted to 6 using NaOH and both solutions contained 0.05 M Nd. HIBA was then titrated into the sample cell. Spectra was measured for many concentrations of HIBA up to a final concentration of 0.2 M. Neodymium's spectra did not display any isosbestic points that would indicate complexation between HIBA and neodymium, even when the concentration ratio was 1:4 for Nd:HIBA.

Since no isosbestic points were observed with HIBA, EDTA was evaluated. A similar approach was taken by placing 0.05 M neodymium nitrate solution in the sample and reference cell then titrating EDTA into the sample cell. Both pH and ionic strength of titrand and titrant were adjusted prior to performing the experiment. The concentration of EDTA ranged from 0 M to 0.15 M. A shift in the neodymium spectra was observed indicating complexation occurring between EDTA and neodymium, as seen in Figure 3-5. When compared to Figure 3-2, a change in the maximum and the shape of the spectrum is easily spotted as the titrant is added, as well as an isosbestic point at roughly 570 nm. Although complexation was observed for this spectra, these data were not further processed using the HypSpec software since this was only done for method development purposes.

Following a similar rationale as in Chapter 2, citric acid was used in order to test the overall UV-Vis spectrophotometry method by recreating the experiment from [58].

In order to recreate the experiment in the available spectrophotometer, some adjustments had to be made. In the paper, the starting volume in the cell was 1.25 ml. However, based on the previous experiments, this small volume was not detectable in the Cary 300 used in these studies. An initial volume of 2.21 ml was needed to obtain a consistent spectra. For this purpose, it was decided that the starting volume would be 2.21

ml and titrant injections would be performed until the cell was full. At this point, some volume would be taken off the cell and the injections up to the final concentration of titrant would be continued. This was taken into account in the calculations needed for the HypSpec data processing later.

This experiment was performed using triplicates of the sample. The cells were kept at 25 ºC and their content was stirred using magnetic bars. Five minutes was allowed between injections before the spectrum was recorded. A total of 24 injections of 0.08 ml of titrant was performed. Figure 3-6 shows only some of the spectra recorded since when trying to plot the 24 spectra the visibility of the plot decreased. It should be clarified that these data are not corrected for absorbance calibration, therefore the spectra does not have its minimum at zero absorbance units. The reason why this calibration was not performed is that this experiment was only done to check the method and instrument performance for complexation studies.

The titrant consisted of 0.1665 M sodium citrate and sodium perchlorate to adjust the solution to 1 M ionic strength. The titrand consisted of 0.0388 M neodymium nitrate and 0.1544 M citric acid plus sodium perchlorate to adjust the solutions ionic strength to 1 M.

Knowing that citrate is invisible in the UV-Vis spectra, this plot shows how the spectra of neodymium is affected by the complexation with the citrate ligand by showing a red-shift in the spectrum. Although this plot only shows data corresponding to one of the samples, the other two samples showed similar spectra and would have resulted in similar HypSpec results.

When these experimental data are compared to the HySS model produced from the

previous published data, Figure 3-7 is obtained. This comparison corresponds only to a single injection of the experiment, injection 11. Twenty-four different figures could be produced in a similar fashion for additional comparisons.

In Figure 3-7, the blue diamond points correspond to experimental data while the red line that fits them, corresponds to the model. The colored spectra correspond to the different species as shown in the legend, in this case, only NdCit, NdCitH and $NdCit_2$ have a significant spectra. As can be seen in the plot, the experimental and the HySS model resulted in very good agreement enabling HypSpec to refine the experimental data to adjust them to the theoretical model and produce stability constants specific for our experiment in a similar way as was done by HyperQuad in Chapter 2. Table 3-1 shows a comparison between the refined constants for our experiment and the reported constants in the peer reviewed publication. There are small discrepancies between the previously reported stability constants and those obtained in this study. The NdCit stability constant disagrees by 7.8%, NdCitH by 8.3%, $NdCit_2$ by 18.2% and $NdCit_2H$ by 24.7 %. As can be seen, HypSpec refined well for NdCit and NdCitH species, but the refinement of the experimental conditions to the model was poor for the other two species. It can also be seen that the standard deviation of NdCitH could not be refined by the software either, which is explained by the fact that there is only a certain number of iterations HypSpec would go through for data convergence before aborting the process. The possible causes of this issue include that $NdCit_2$ and $NdCit_2H$ may be spectroscopically inert species, which would cause the free metal and ligand concentrations to not be at their true value and therefore the HypSpec calculation of the stability constants to be affected. A more exhaustive discussion of these issues is addressed extensively in the section entitled ‘Absorption

spectrophotometry and equilibrium analyses' in [58].

Once the UV-Vis spectrophotometry method was proven successful with the previously published results, its role in stability constant and pK_a value determination for enterobactin was considered. Further discussion about this will follow in Chapter 5, which focuses on enterobactin experiments.

Table 3-1. Comparison of reported and experimental constants refined with HypSpec

Species	Stability constant, β	
	Reported value [58]	**Refined experimental values**
NdCit	7.0 ± 0.2	6.4566 ± 0.5044
NdCitH	9.6 ± 0.1	8.8011 (Standard Deviation could not refine)
$NdCit_2$	9.7 ± 0.7	11.4693 ± 0.6405
$NdCit_2H$	12.1 ± 0.1	15.0943 ± 0.6907

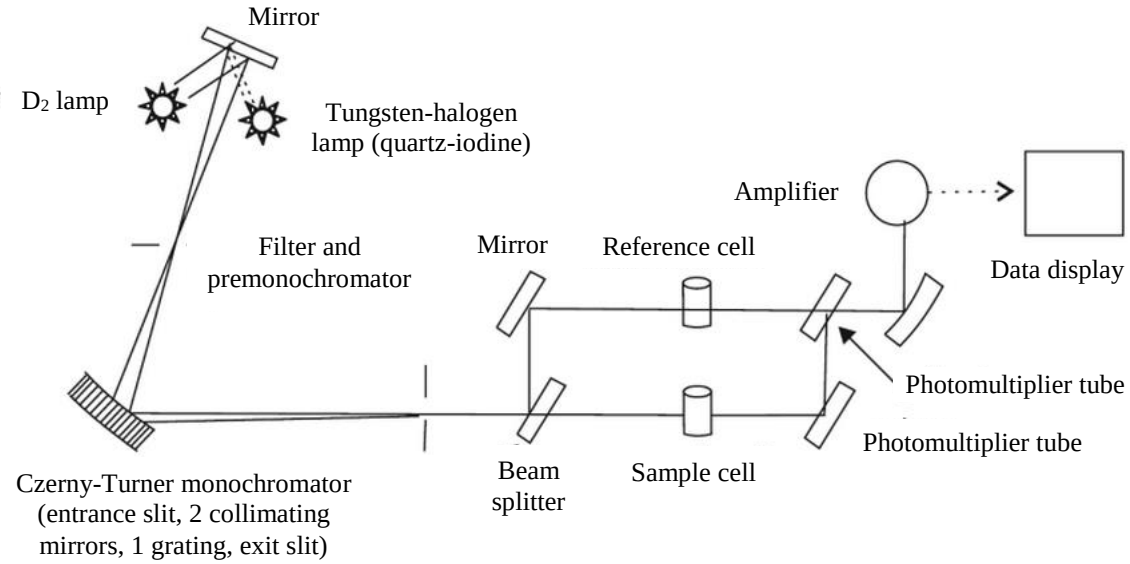

Figure 3-1. UV-Vis spectrophotometer. Modified from [69]

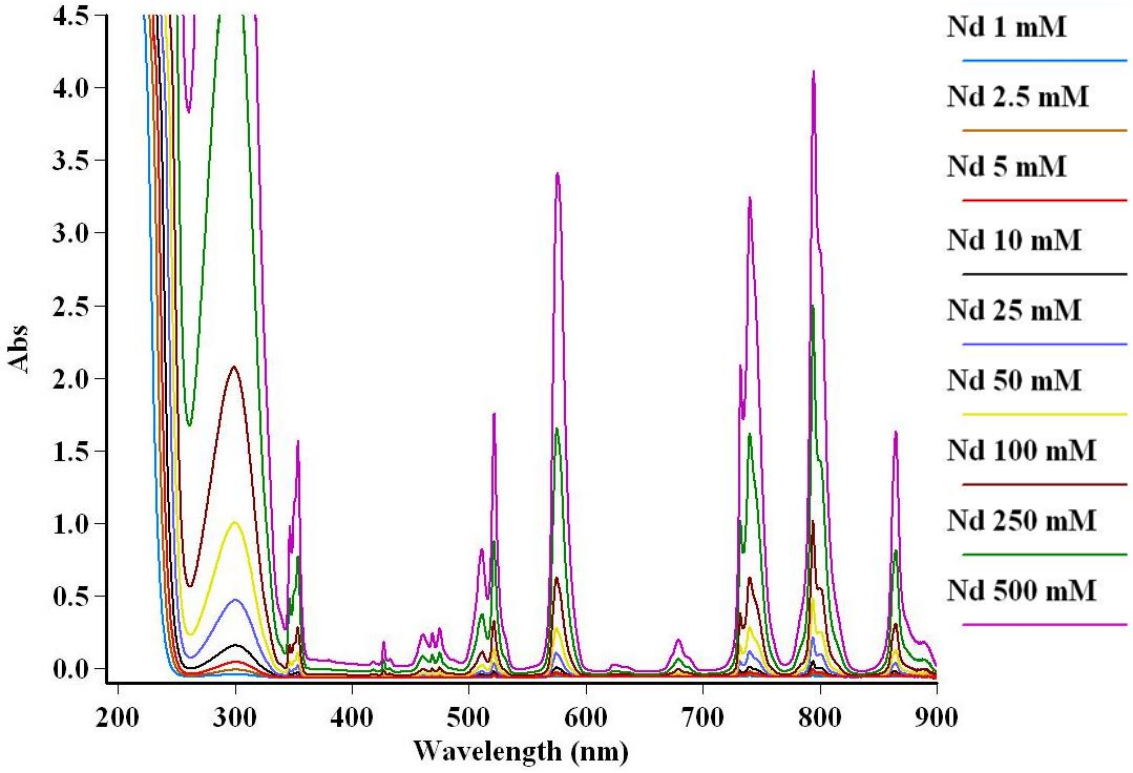

Figure 3-2. UV-Vis spectra of neodymium in different concentrations

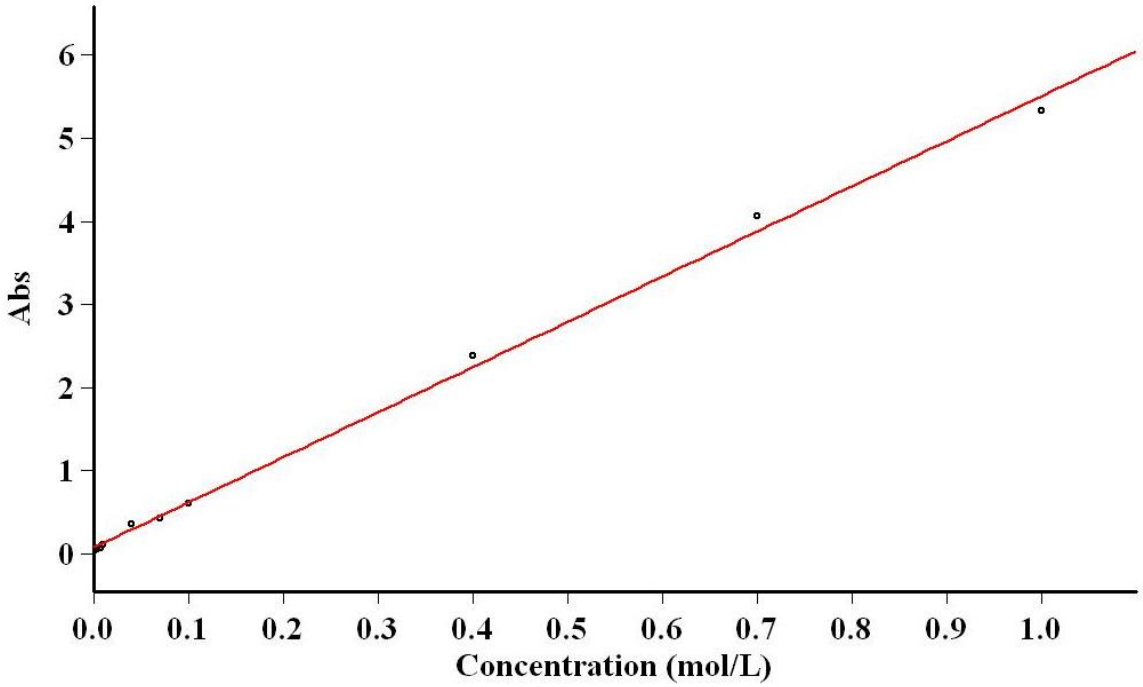

Figure 3-3. Calibration curve for neodymium in the UV-Vis spectrophotometer

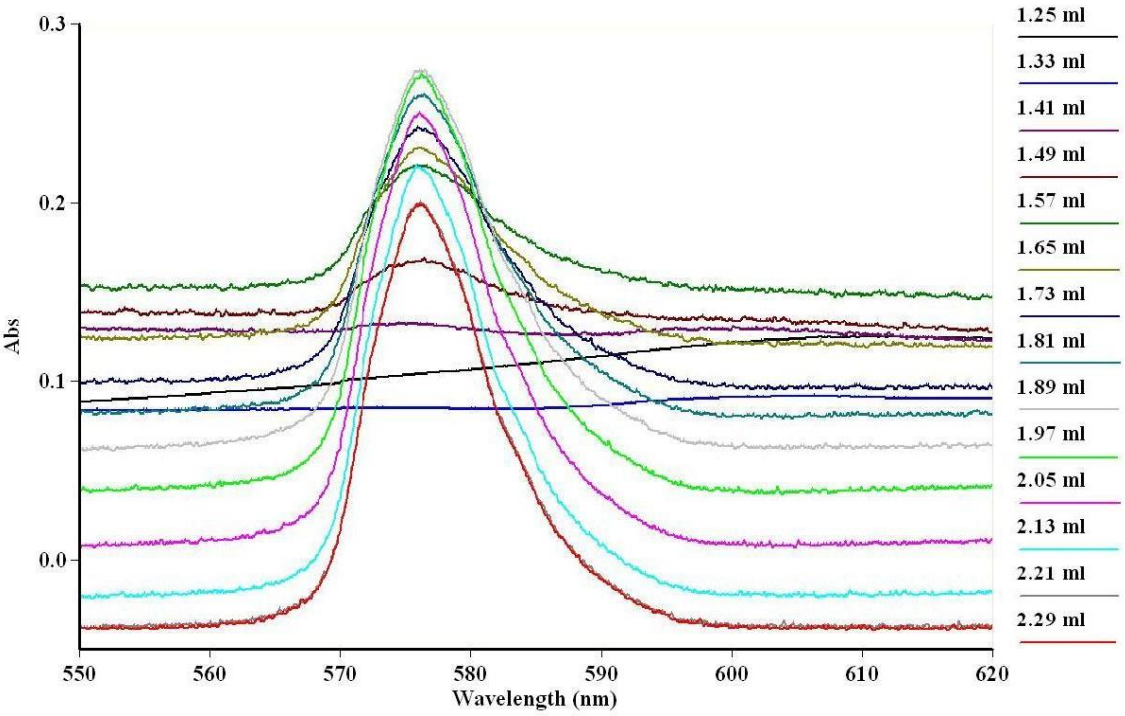

Figure 3-4. Liquid height experiment for 1 cm path length UV-Vis spectrophotometer

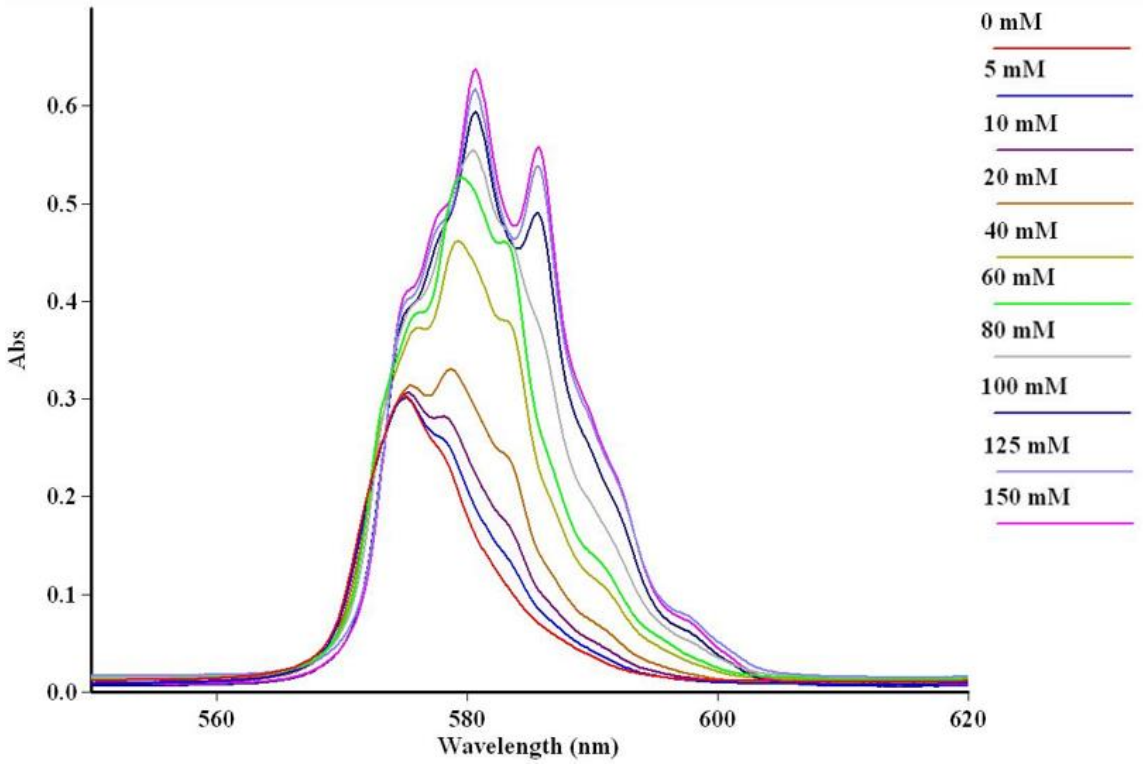

Figure 3-5. Change of UV-Vis spectra of neodymium as EDTA is added

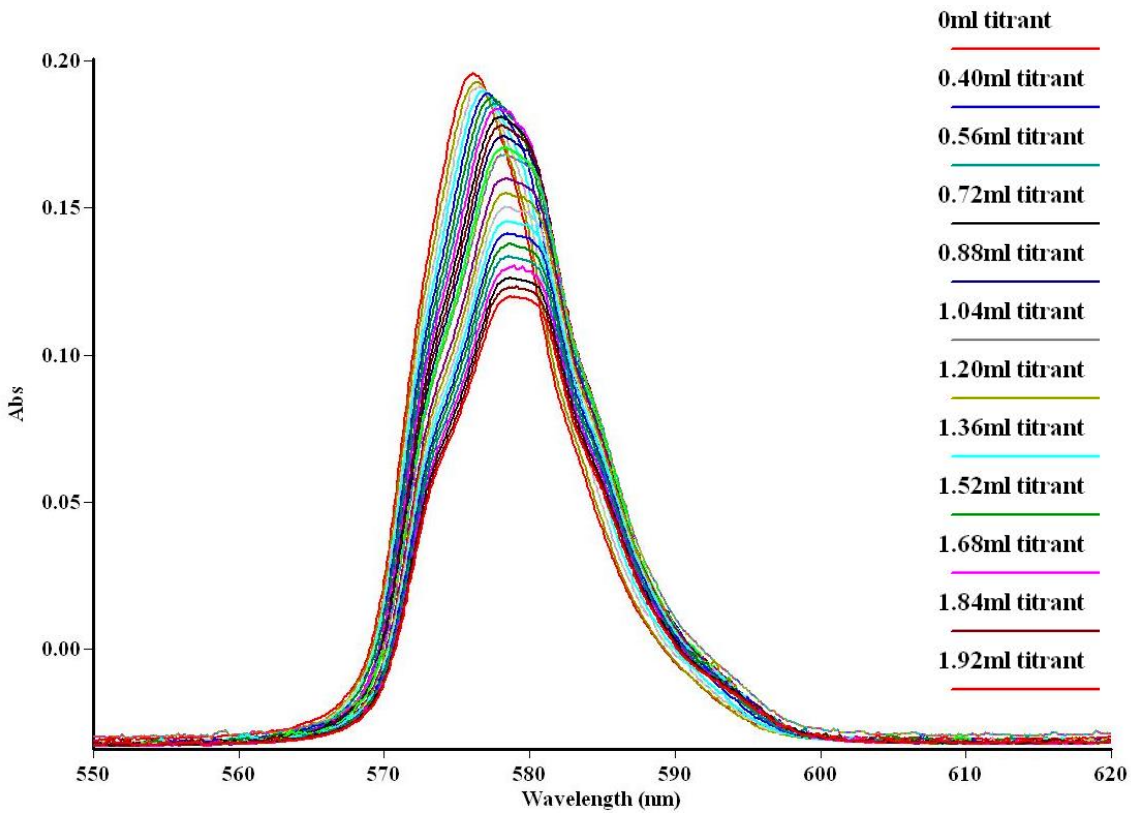

Figure 3-6. UV-Vis spectra for neodymium-citrate complexation

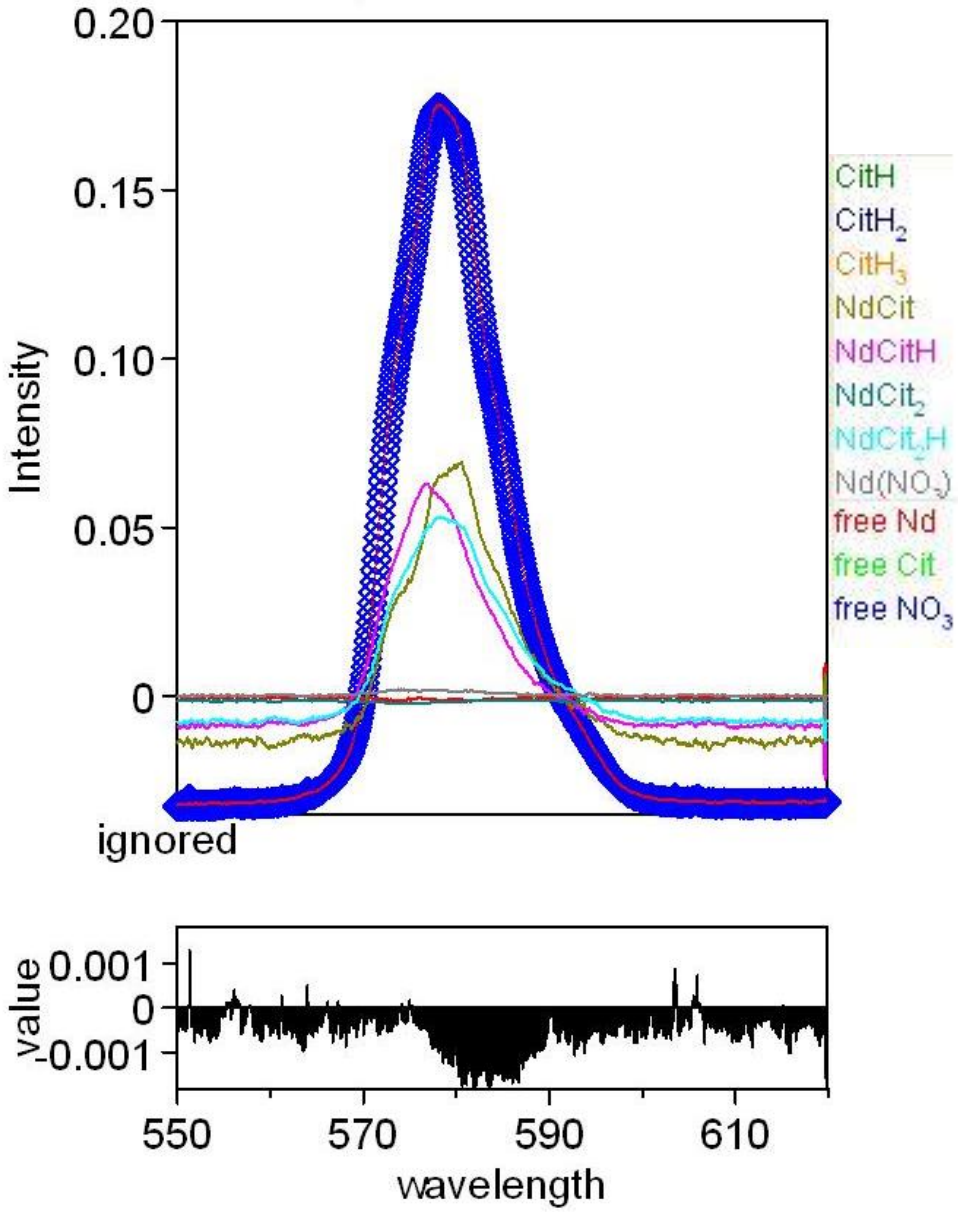

Figure 3-7. HypSpec results comparing the HySS model and the experiment

CHAPTER 4

ISOTHERMAL TITRATION CALORIMETRY

4.1 Fundamentals of calorimetry

The following discussion of principles of calorimetry and its application to stability constants and pK_a value determination is done following the training materials given by TA Instruments, the manufacturers of the calorimeter used for this study.

Calorimetry by definition is the measurement of heat properties as a function of time and temperature. Taking into account that all chemical and physical processes produce or absorb heat, this heat can be quantified and used to characterize the process using calorimeters. In this study, heat flow was measured in units of μJ/s.

Calorimeters are classified according to their sensitivity and sample size. The most sensitive calorimeter is the nanocalorimeter, which is able to detect heat flow changes in the nW level. Because of its extreme precision, this calorimeter only holds very small sample sizes with a maximum sample size of 4 ml. In this study, a TA Instruments TAM III nanocalorimeter was used for all experiments. A picture of the setup in the laboratory can be seen in Figure 4-1.

In the calorimeter there are two rods, the sample rod (A) and the reference rod (B). Their role in heat flow measurements will be later explained in this chapter. The titrant syringe is inserted in the cannula of the sample rod and goes to the bottom of the cell.

The titrant is injected using a mechanical syringe pump. Another cable connects the sample rod to the controller and the stirrer. The stirrer is directly in contact with the shaft that holds the propeller in the sample cell allowing good mixing of the sample. Both the stirrer and the syringe pump can be controlled using TAM's software, and the syringe also has a manual keyboard integrated in the pump that can be used to control it as well. This software is also used to run experiments, edit results and evaluate data. Surrounding the calorimeters is an oil bath that thermostats the temperature of the calorimeter. The temperature can range from 15°C to 120°C. For all experiments discussed in this thesis, the temperature was maintained at 25°C. This temperature is controlled as shown in Figure 4-2.

In calorimetry, there are two main variables to take into account: rate of heat production (exothermic or endothermic), and rate of heat exchange (i.e., the rate of heat flow transmitted from the sample and the surroundings). The only variable that can be physically measured is the rate of heat exchange but this is only equal to the rate of heat production in steady state conditions, which is why calibrating the calorimeter is necessary to get reliable measurements during an experiment. The heat flow displayed in the calorimeter screen is proportional to the rate of reaction in these conditions. Equation 4-1 shows how the heat flow recorded as it relates to the thermodynamic, kinetic and analytical information of the reaction.

$$\frac{dQ}{dt} = \Delta H \cdot k \cdot c \qquad (4\text{-}1)$$

In this equation, dQ/dt is the heat flow signal, ΔH is the enthalpy change of the reaction, k is the reaction rate and c is the concentration of the reagent. This equation explains how the heat flow is directly proportional to the concentration of the reagent, but

this relation is also affected by the enthalpy and order of the reaction.

In order to reduce the noise of the measurement, a twin channel calorimeter can be used, like the one used in this study. This type of calorimeter uses a sample and a reference cell.

After the temperature has been set in the heat sink, two thermocouples are used to keep the temperature in both sample holders, T_S and T_R, as close as possible to the surrounding heat sink. In each of the sample holders, the respective reaction's heat of production are being released, Q_R and Q_S, and each of the cells' content also has different heat capacities, C_S and C_R, which need to be considered in the heat balance equations. Between the sample holder and the surroundings of the calorimeter, heat is being transferred, and the main variable to account for this heat transfer is the heat conductance of the medium, k_S and k_R, respectively, for each sample holder. The heat conductance depends on the heat capacity C, a known property for most materials at different temperatures, and a time constant τ, which can be measured with a calibration of the instrument

Taking all of these variables into account, the heat balance equation for each of the sides of the calorimeter can be written and subsequently, a global heat balance equation for the system can be deducted.

Sample side:

$$\frac{dQ_S}{dt} = k_S(T_S - T_0) + C_S\frac{dT_S}{dt} \tag{4-2}$$

Reference side:

$$\frac{dQ_R}{dt} = k_R(T_R - T_0) + C_R\frac{dT_R}{dt} \tag{4-3}$$

Since the TAM system works with a high heat capacity and thermal stability, it can

be assumed that $C=C_R=C_s$ and $k=k_R=k_S$ and therefore a global heat balance equation can be written as:

$$\frac{dQ_S}{dt} = k(T_S - T_R) + C\frac{d(T_S - T_R)}{dt} \quad (4\text{-}4)$$

It is important to note that for isothermal calorimetry it is not necessary to know the heat capacity of the sample, since the instrument does not measure the change in temperature but the rate of heat production directly, which is proportional to the overall reaction rate as in Equation 4-1.

It is important to try to make the reference cell and its content as close to the sample cell as possible. Since titrations typically have a low response in heat flow, identical cells were used with identical sealing systems (1 ml hastelloy cells with circlip caps), and the same exact solution was placed in the reference and sample cells for each of the experiments. Special attention was also paid to the titrant volume, so that the added titrant volume was not big enough to unbalance the sample and reference cell. For example, 250 µl would be titrated into the sample cell to make a total volume of 1 ml.

A dynamic calibration was performed before every experiment to adjust the time constant. Since every time an ampoule is loaded, the time constant of the calorimeter increases. This type of calibration is performed when the response of the reaction is less or around the same as the time constant of the system, i.e., fast processes. In addition, every 3 months due to the ageing of the semiconductor thermopiles, a General Performance Test (GPT) also needs to be completed, which includes a heat flow calibration for slower processes. All calibrations use an internal electrical heater and apply a known calibration power to the calorimeter. Since the temperature probes measure voltage that is then converted to the corresponding rate of heat production, this calibration helps with the

accuracy of the conversion and it also accounts for heat losses.

In an analog way, two major heat measuring modes can be set: heat flow mode, which has a higher sensitivity but requires longer time scales, and dynamic heat flow mode, which takes into consideration the thermal inertia of the calorimeter. For calibrations and General Performance Tests (GPT), the heat flow mode would be activated, but for titration experiments the dynamic heat flow mode will be the one selected.

Since calorimetry is a nonspecific technique, the calorimeter will record the heat flow from all the physical and chemical processes that occur in the experiment. For this purpose, it was necessary to run blank experiments to account for all the heat flow produced from all the processes that were not the chemical reaction of interest. For example, dilution of the drop of titrant in the titrand or the stirring heat must be accounted for in the blank experiments. Blank experiments were analog in every way to experiments with samples except that the solutions in the cells included all the chemical components apart from the molecule of interest, i.e., citrate, EDTA or enterobactin. Therefore, when the blank heat flow was subtracted from the sample heat flow, it could be said that the remaining heat was due only to the protonation/deprotonation or complexation of the ligand of interest.

Before starting any experiment or calibration, the calorimeter's signal must be stable. Stability in the signal is reached sooner or later depending on the sample size, its prehistory (i.e., if it was stored close to the experiment's temperature then the signal will stabilize faster), and its composition (i.e., samples containing volatile components such as methanol might require more time for the signal to stabilize.)

4.2 Application to pK_a or stability constant determination

For the study of molecular interactions such as ligand binding, complexation or deprotonation, Isothermal Titration Calorimetry (ITC) is vastly used. In ITC, a certain temperature is setup, in this case 25 ± 0.1 ºC, and the heat flow is measured as the titrant is added in repeated injections at certain time intervals through a syringe to the sample in the sample cell. The heat effects of the injections are observed as peaks in the thermogram displayed by the calorimeter where the heat flow in μJ/s is plotted versus time. Negative peaks indicate endothermic events while positive peaks indicate exothermic events.

Binding in general, protonation or complexation included, is characterized through a thermodynamic constant (K), a certain stoichiometry (n), and the reaction's thermodynamics. Thermodynamics are described using several variables. ΔH measures the heat released or absorbed, ΔG measures the equilibrium constant, ΔS measures the order of the system and ΔC_p measures the temperature dependence of ΔH. All these variables are related using the following set of equations.

$$\Delta G = -RT \ln K \tag{4-5}$$

$$\Delta S = \frac{(\Delta H - \Delta G)}{T} \tag{4-6}$$

$$\Delta C_p = \frac{d(\Delta H)}{dT} \tag{4-7}$$

ΔH can be directly determined in all cases using ITC, and the stability constant can be determined as well via ITC provided that the concentrations and magnitude of K are in certain ranges. To determine ΔH, it is necessary to subtract the dilution experiment peaks from the sample experiment peaks and then the enthalpy of the reaction would be the sum of all the injections' peaks. If both K and ΔH of the reaction need to be measured in the same experiment, then very low concentrations are required in order to measure stability

constants of very strong complexes, as explained in [1]. In general, the total concentration of the metal should be typically 10 to 100 mM and the K value should be 10^3 to 10^9 M^{-1}. This specific range of concentrations has to release a strong enough heat flow signal to be detected by the calorimeter and it also may or may not be possible to alter the experiment's temperature according to the solubility limit of the substance. Therefore in most cases, K values are determined using other techniques such as spectrophotometry or potentiometry.

From known values of K and ΔH, it is easy to determine ΔG and ΔS using Equations 4-5 and 4-6. In order to determine ΔC_p, several experiments at different temperatures can be performed and a plot of T vs ΔH will yield ΔC_p as the slope of the line. It is worth mentioning that although ITC is both suitable for the characterization of protonation/deprotonation reactions and complexation reactions, it has extensively been used in complexation but has barely been used for pK_a determination.

In a similar way as potentiometry and UV-Vis spectrophotometry, in order to process the experimental data to obtain pK_a values and stability constants, HypΔH software can be used. With the heat flow measurements, the initial concentration of the analyte, and pH values of the solutions in the syringe and cell, both ΔH, K and ΔS can be obtained for the experiment. A suitable model of the system should be develop in HySS first, as described also in Chapter I. HypΔH then takes the experimental data and refines them to adjust to the theoretical HySS model in the best way possible. TAM software also has a tool for this sort of binding analysis, but if the model is too complicated and several species are involved in, this tool would be insufficient, as in the case of our study.

4.3 Procedure and experimental considerations

In calorimetry, the titrand containing the ligand is adjusted to a certain pH value and ionic strength and placed in both the reference and the sample hastelloy cells. Then the propeller and syringe tip are adjusted in the sample cell before the cells are closed using the circlips and lowered slowly into the calorimeter to minimize large temperature variations. The titrant solution in the syringe has been adjusted for pH and ionic strength and is loaded in the syringe pump. The stirring is started while waiting for signal's stability. In the meantime, since the calorimeter is fully automatized, after both solutions have been prepared, the titration can be controlled using a computer and the TAM software, in this case, TAM assistant. A new experiment is setup and all the information related to the experiment (i.e., the number of injections, injection time, injection volume and the time between injections) is specified. Once this is done, it is only necessary to wait for signal stability to begin the experiment. TAM will automatically perform a dynamic calibration first (if selected by the user) and then proceed to the titration experiment. Once the experiment has finalized, it is necessary to press the finish button on the same experiment tab so that the results are saved. Then they can be analyzed using TAM's software or other TA instruments software such as NanoAnalyze, to export the data as needed.

4.4 Data produced and how they helped in the method development process

Analogous to the previous techniques, the same experiment as in [58] was recreated in this laboratory to verify proper use of the instrument. On the different trials, some factors of importance due to the high sensitivity of the calorimeter became evident. The most

remarkable ones were the extreme care that was needed in the preparatory steps of the experiment in order to obtain a good baseline in the experiment, and the amount of time between injections. It was found that any less than 15 minutes between injections would be too little time for the signal to return to baseline using dynamic mode. By reading the paper, it appears as if the authors were using heat flow mode with 10 minutes between injections. However, when doing this, we found that the signal did not have enough time return to baseline in the experiment of interest and a minimum time between injections of 20 minutes was needed because heat flow mode does not account for the thermal inertia of the calorimeter. For time economy reasons, dynamic mode was used for ITC experiments and 15 minutes was allowed between injections.

After these considerations, an experiment to determine the pK_a values of citrate was performed. The temperature was set at 25 ºC and the ionic strength of titrand and titrant was adjusted to 1 M using sodium perchlorate. For citrate's pK_a the titrand solution had a concentration of citrate of 37.6 mM, a concentration of protons of 12.7 mM and a volume of 0.8 ml. The titrant solution was composed of a mixture of 400 mM perchloric acid and 600 mM sodium perchlorate. The stirrer rate was set to 80 rpm and maintained with a gold propeller. The injection volume was 5 microliters, the injection time was 10 seconds, and 10 minutes was allowed between injections. The total volume titrated in summed up to 0.2 ml. A dynamic calibration was performed before each experiment. The raw data from the calorimeter for the sample experiment are shown in Figure 4-3. These data are not corrected for dilution.

Data corrected for dilution can be input into HypΔH software for processing and determining thermodynamic information. The HySS model needs to be previously created

and input in HypΔH as well. In this case, the model was written based on the constants reported on the peer-reviewed paper.

Once these data are input, an abundance of information can be obtained from the refinement. If the heat of reaction of each of the species involved in the model is unknown, a refinement can be performed for obtaining them. A refinement can also be obtained at the same time for the constants if they are set as unknown. In the case of unknown constants, the software will try to refine both the enthalpies of each species and their equilibrium constants at the same time to try and fit the experimental data. Figure 4-4 shows the plot HypΔH produces with the experimental data shown as diamonds and the HySS model shown as + points. The different species involved are also displayed in color. As the titre volume is added, the pH changes and therefore their concentration changes as well.

Once the data have been plotted, the refinement can be performed. In this case, only the enthalpy of the different species was refined since this is what was done in the paper that was recreated. HypΔH also allows us to determine the values for TΔS, as in the paper, but since these values are not refined by the software, but calculated using the same formulas as presented in this chapter, they will not be discussed in this analysis. Results can be compared to the ones reported in the literature as in previous sections and can be seen in Table 4-1.

The reported and experimental data do not agree completely. CitH enthalpy disagrees by 30%, $CitH_2$ disagrees by 19 % and $CitH_3$ disagrees by 11 %. It can be seen that the error highly depends on the species that is being considered, but it is worth mentioning some possible sources of error. The reported constants were determined with standardized solutions. In the experiment this standardization was not performed since this

process is time consuming and strenuous and the data were only used to check that our methodology was correct in using the equipment and not for publishing purposes.

For the same reason, no statistical analysis was performed in these data (i.e., no replicates were performed) and therefore, it could be that the experimental data were not as accurate as initially thought. However, since the enthalpy values are in the order magnitude of the previously published values, experimental focus moved to enterobactin.

Since the concentrations managed in this experiment were far too high to use in the case of enterobactin, another set of experiments was performed to see the concentration influence in the peaks displayed by the calorimeter. In order to see this concentration influence, the neodymium-citrate experiment described in [58] was replicated. The first experiment was performed with the same concentration values as reported in [58], a second experiment was done afterwards where all concentrations were lowered by a factor of ten with respect to the original paper and finally a third analog experiment was done with all concentrations lowered by a factor of a hundred with respect to the original concentrations reported in the paper. The temperature was set at 25 ºC and the ionic strength of titrand and titrant was adjusted to 1 M using sodium perchlorate. The titrand solution had a concentration of neodymium of 7.4 mM, a concentration of citrate of 50 mM, a concentration of protons of 56.6 mM and a volume of 0.8 ml. The titrant solution was composed of a mixture of 400 mM perchloric acid and 600 mM sodium perchlorate. The stirrer rate was set to 80 rpm and maintained with a gold propeller, the injection volume was 5 microliters, the injection time was 10 seconds and 10 minutes was allowed between injections. The total volume titrated was 0.2 ml. A dynamic calibration was performed before each experiment. All the variables remained the same for the three experiments apart

from the concentrations. Since the first few injections are usually neglected to account for possible syringe tip dilution, after taking the first three injections out, Figure 4-5 shows the peak area versus the injection number for the experiment set. These data are not corrected for dilution.

Peak area is the standard variable for data analysis when it cannot be done using tools such as HypΔH, since when replicating an experiment peaks can vary in height or thickness but their area should be the same. As can be seen, peak area follows the same trend in all experiments although this trend may seem unclear as the concentrations is lowered due to the magnitude of the axis. It is also proportional to the concentration, higher concentrations give higher peak areas, but concentration and peak area do not seem to follow the same factor of proportionality (concentration increases by 10, peak area increases by approximately 3). This shows good agreement with what was extracted from Equation 4-1; there is a proportionality, but the factor of proportionality is not the same since heat flow also depends on kinetics and order of reaction.

Once these experiments were performed, the calorimetry method followed was proven successful with already reported data in the method development process. Next, its role in stability constant and pK_a value determination for enterobactin was considered. Further discussion about this will follow in Chapter 5, which focuses on enterobactin experiments.

Table 4-1. Reported and refined experimental enthalpy values using HypΔH

Species	Enthalpy ΔH (kJ mol^{-1})	
	Reported value [58]	Refined experimental values
CitH	-0.42 ±0.06	-0.29 ±0.06
$CitH_2$	-4.33 ± 0.06	-3.47 ± 0.05
$CitH_3$	-8.04 ±0.08	-7.08 ± 0.05

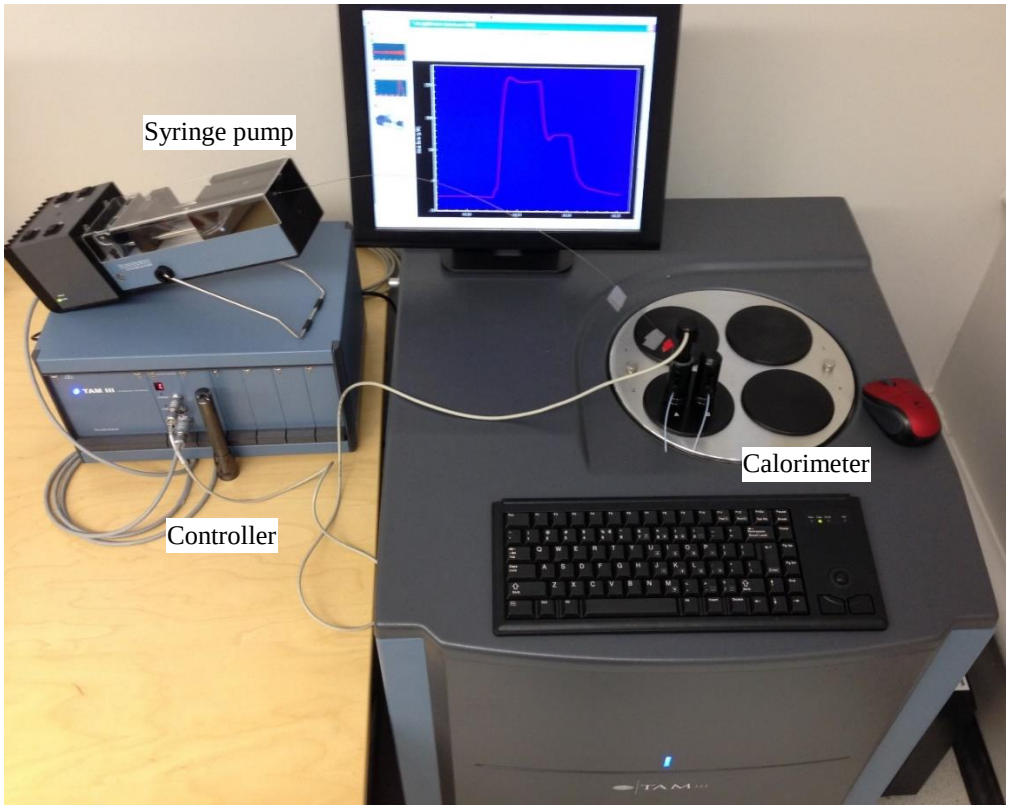

Figure 4-1. Nanocalorimeter TAM III

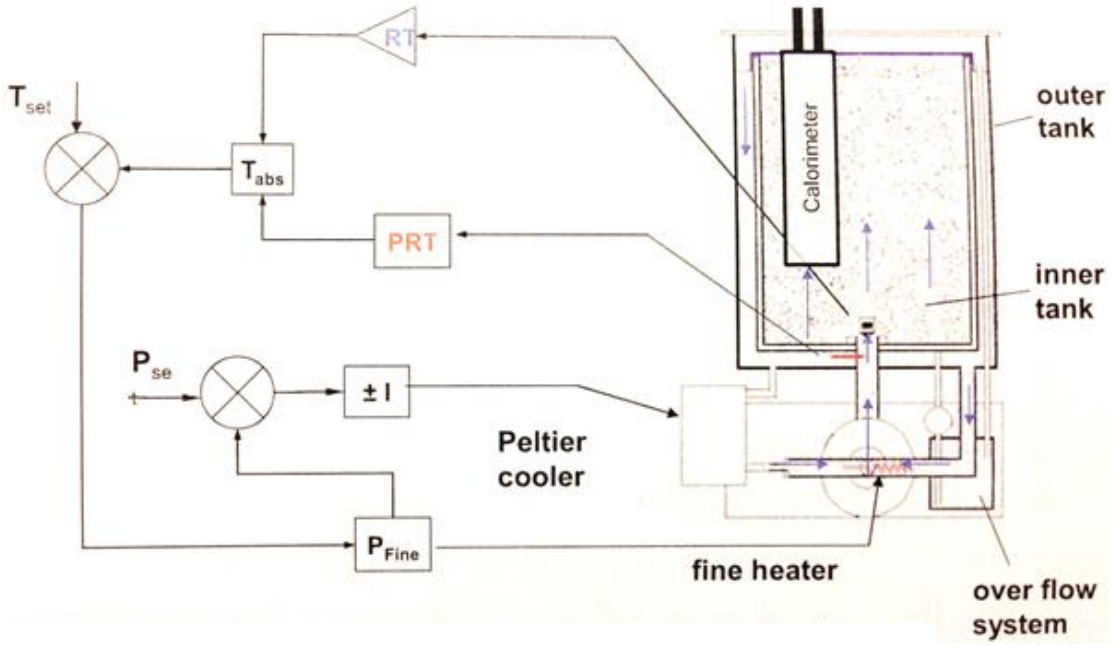

Figure 4-2. Temperature control as used in TAM III. Modified from TA Instruments' training materials

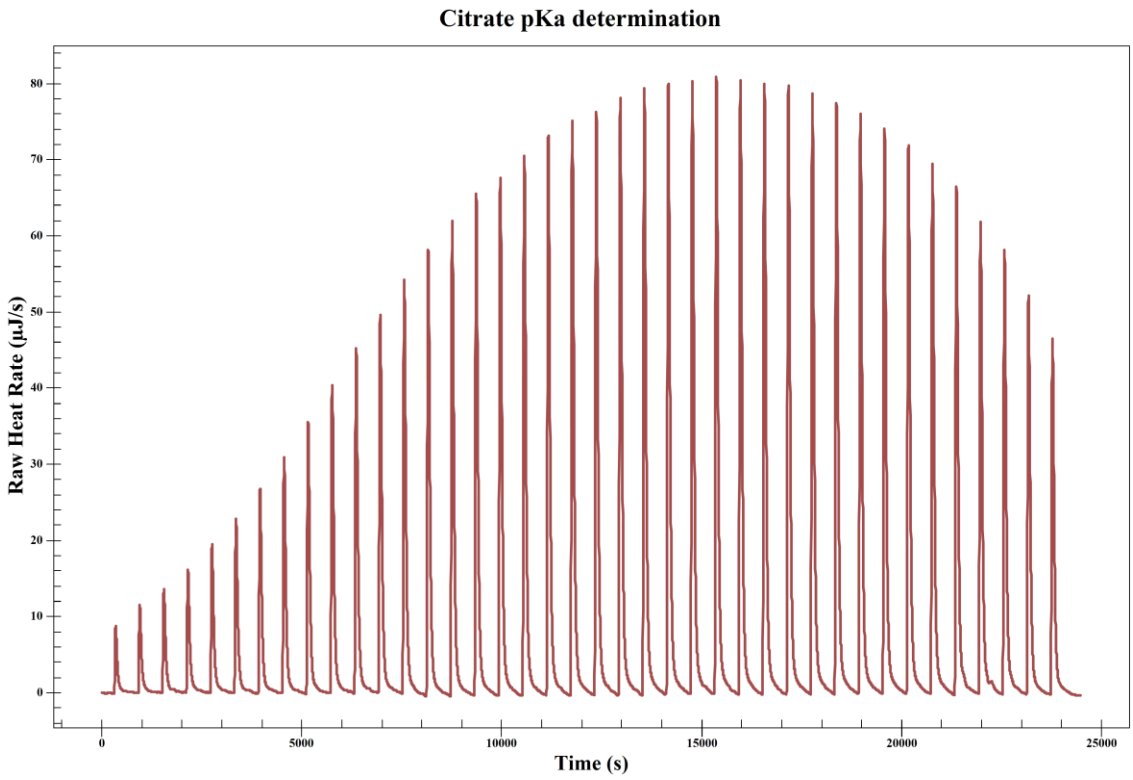

Figure 4-3. Raw calorimeter data for citrate pK_a determination

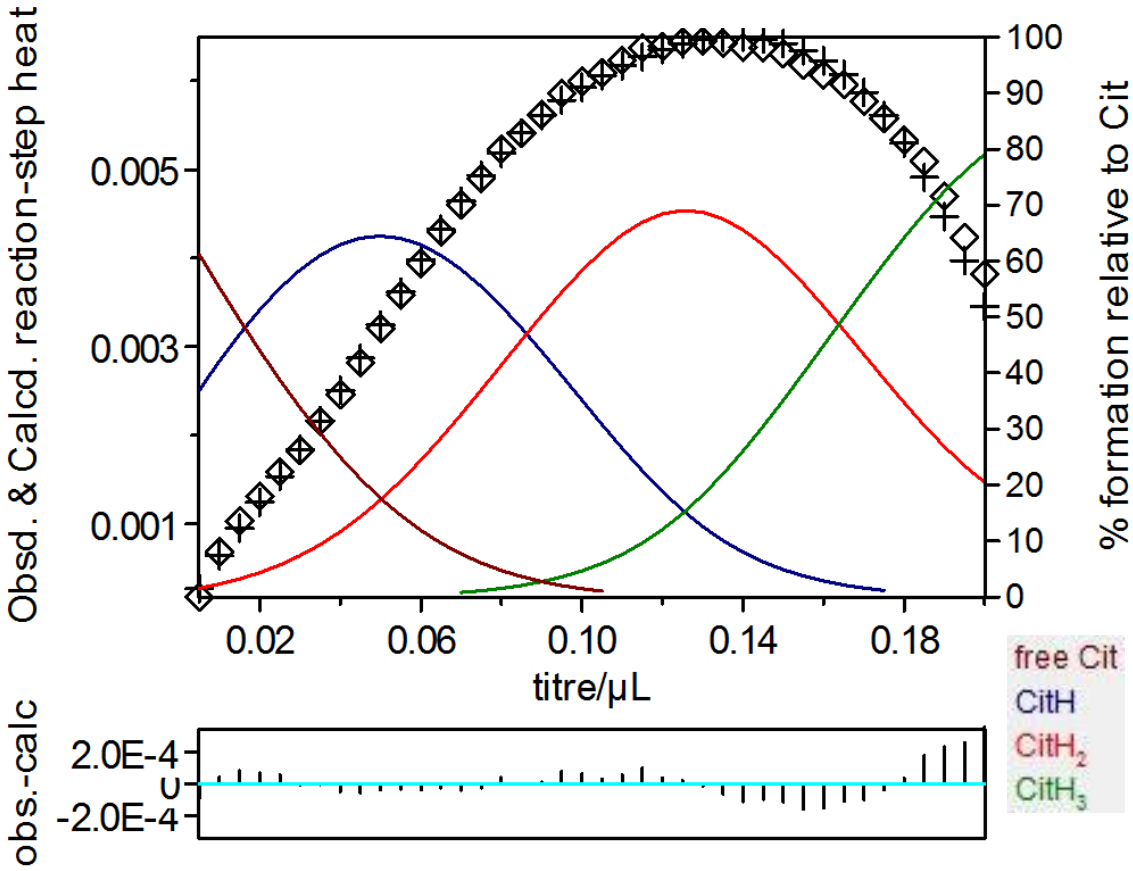

Figure 4-4. HypΔH results for citrate pK_a determination

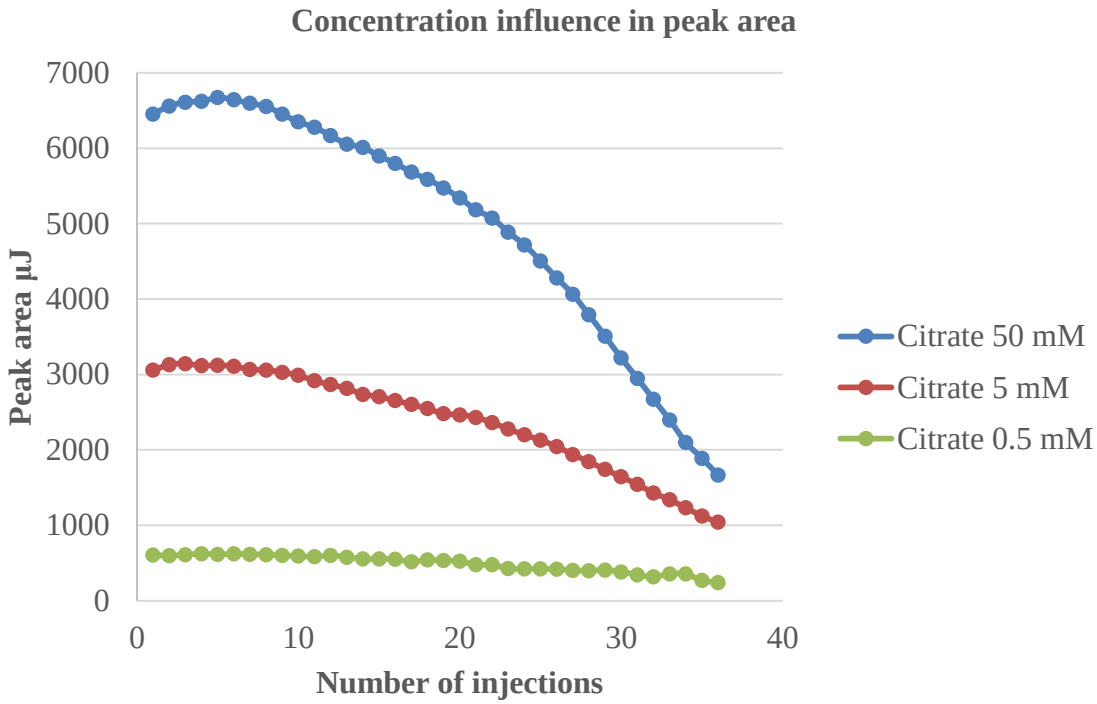

Figure 4-5. Peak area magnitude influenced by concentration

CHAPTER 5

ENTEROBACTIN RESULTS

5.1 Enterobactin

Enterobactin is a siderophore produced by *Escherichia coli*, a very common bacteria in the environment [70]. A 2D representation of this molecule can be seen in Figure 5-1. Enterobactin was chosen for this study because it has low pK_a values reported, which means it would easily deprotonate and it could therefore be a potential leaching agent for acid bioleaching [71]. Having low pK_a values would also facilitate working at comfortable ranges of pH avoiding extreme pH exposure for the laboratory equipment.

In order to make enterobactin soluble, it is necessary to use organic solutions such as methanol in a volume proportion around 3% to that of water. This already poses some challenges for working with enterobactin, since as mentioned in Chapter 4, solutions with high volatility such as methanol make reaching stability in the signal more difficult in the calorimeter. Moreover, aqueous solubility of enterobactin itself is only approximately 0.1 mM [72], which forced us to work with very low concentrations in the experiments performed.

When exploring what has been done up to date with enterobactin in complexation studies, few peer-reviewed publications were found, even though as said before, this is a very common bacteria.

For pK_a determination, only two peer-reviewed publications were found [73] [71] and for complexation with trivalent metals, only three publications were found [71] [74] [75]. In this literature, only complexation constants between enterobactin and trivalent aluminum, iron, gallium, indium and scandium were reported. Regarding pK_a determination, only three out of nine possible pK_a values were reported at 25 ºC and 0.1 M ionic strength maintained using KCl: $pK_{a4} = 8.55 \pm 0.09$, $pK_{a5} = 7.5 \pm 0.2$ and $pK_{a6} = 6.0 \pm 0.5$. Technique wise, according to the literature, all of these complexation constants and pK_a values were determined using the same technique, UV-Vis spectrophotometry.

From this literature review, it is clear that a lot has yet to be done with enterobactin in order fully characterize it as a complexing agent. From all the nine common techniques for pK_a and complexation constant determination addressed in Chapter 1, only one of them was applied to enterobactin; six of enterobactin's pK_a values have yet to be determined and only complexation constants with five trivalent metals have been reported. None of these trivalent metals are gold, copper or uranium, the most common metals extracted via bioleaching and enterobactin has never been reported to be used as a complexant in bioleaching, despite having the chemical potential for it.

Knowing this, the focus of this study was developed: characterizing new pK_a values of enterobactin, confirming the pK_a values that have been reported using other techniques and potentially determining enterobactin's stability constant with neodymium, a trivalent metal that can serve as a chemical analog to the trivalent actinides.

5.2 Results with UV-Vis spectrophotometry

Since according to the literature, UV-Vis spectrophotometry is the most extensively used technique with enterobactin, the first experimental work was performed trying a similar approach as in [71] with aluminum, iron, indium, gallium, scandium, but now using neodymium. The goal was to determine a stability constant between neodymium and enterobactin.

It is worth mentioning a significant difference between neodymium and the other reported trivalent metals in the paper: neodymium does have a UV-Vis spectra by itself, as seen in Chapter 3 and previously reported in [68] while aluminum, iron, gallium, indium and scandium do not. The UV-Vis spectra seen during the experiments performed in [71] belonged to enterobactin, and as the siderophore complexed with the different trivalent metals, its spectra shifted as a consequence of the metal-ligand binding reaction, as explained in detail in Chapter 3. This shift lead to the appearance of isosbestic points, which allowed the characterization of stability constants of the different metals with enterobactin.

In this case, both the metal, neodymium, and the ligand, enterobactin, have a characteristic UV-Vis spectrum. Therefore, it could potentially be possible to observe both the neodymium spectra shifting as the complexation reaction happens and the enterobactin spectra shifting with the complexation as well. Since the neodymium spectrum is well known due to all the experiments previously performed and detailed in Chapter 3, first we tried to see a shift in neodymium spectrum.

Because enterobactin is only soluble up to 0.1 mM in aqueous solution, anticipating a one-to-one stoichiometry, solutions with different neodymium concentrations starting at 0.1 mM and up to 1 mM were scanned through the UV-Vis spectrophotometer. This was

done with the purpose of knowing at which concentration was neodymium's signal consistent with its well-known spectra from previous experiments. Figure 5-2 shows these data.

As can be seen from the figure, not until the concentration of neodymium is around 1 mM does the signal resembles the characteristic neodymium spectra. This means that the concentration of neodymium in the cell would need to be more than 6-fold the concentration of enterobactin. Because enterobactin's concentration would be so much smaller than neodymium's, it would not be possible to see a shift in neodymium signal provoked by enterobactin.

Since enterobactin is also UV-Vis sensitive, an experiment was done to see if this signal was able to be detected with our instrument. It is worth saying that the signal from 0.1 mM enterobactin was already detected in [71] experiments, but as opposed to their case and recalling Chapter 3, in our setup it was only possible to work with 1 cm path length cells. In [71] they used both 1 cm and 10 cm path length cells, which according to Beer-Lambert's law would have equivalent effects as incrementing the concentration of the sample by 10. Since this is not specified in the paper, the 0.1 mM enterobactin signal they reported could have been detected using longer cells. Figure 5-3 shows a trial of enterobactin 0.1 mM concentration in a 1 cm path length cell and the signal recorded compared to water and the selected buffer, MES.

As can be seen from the figure, enterobactin at 0.1 mM concentration does produce a signal that can be recorded by the UV-Vis spectrophotometer using 1 cm path length cells. This signal is well distinguished from the signal produced from water and from the buffer selected for pH adjustment, MES. MES is also sensitive to UV-Vis light as explained

in [71], but as can be seen in the figure, the influence in signal compared to enterobactin's influence is negligible.

Because the signal check for enterobactin was successful, an experiment analog to the one carried out in [71] was performed to see if a shift in the spectra was observed as a consequence of complexation with neodymium. Titrand solutions were made of 50 μM enterobactin from a stock solution in methanol, 50 μM neodymium from a stock solution of neodymium nitrate and 5 mM MES, a buffer that would keep the solution around pH 6. All were diluted with water up to 2.2 ml. Ionic strength was maintained at 0.1 M with NaCl and the cell was stirred and maintained at 25 ºC. Titrant solution containing 1 M HCl was added in 10 μl injections allowing 5 minutes of stirring between injections. Figure 5-4 shows some of the data obtained for the experiment, since showing all the injections' spectra will create visibility problems in the plot.

From the figure it is clear that no isosbestic points were distinguished and therefore no stability constants for enterobactin-neodymium could be extracted from the experimental data. It is possible that only weak binding between neodymium and enterobactin at MES pH buffering levels (5.5-6.7), the short cell path length, and solubility limitations of enterobactin, made it difficult to observe complexation with this technique.

5.3 Technique discrimination

In UV-Vis spectrophotometry, the metal of interest for enterobactin complexation was tested and its stability constant with enterobactin could not be determined with the experimental data collected. In addition, no new pK_a values of enterobactin were likely to be found using UV-Vis spectrophotometry in the experimental conditions available in our

laboratory. This was deduced based on the fact that previous literature [71] was only able to determine three pK_a values with similar conditions as the ones of our laboratory and the same technique.

As of potentiometric titrations, a clear limitation was noticed regarding the amount of volume needed to confidently determine end points in the titration. For temperature control purposes, a thermostat vessel is needed for complexation studies. The smallest available jacketed vessels had a minimum volume of 5 ml, which for a product with a high economical value such as enterobactin represents an excessive amount of volume per experiment. Smaller volumes of enterobactin could be titrated for pH monitoring purposes using the potentiometer but the end points identified by the software will not be reliable. It is also worth mentioning that previous studies have mentioned that determining protonation and stability constants of enterobactin have been difficult because a relatively high concentration is needed in potentiometry and enterobactin precipitates over 0.1 mM in aqueous solution [75].

Regarding ITC, multiple studies have been done regarding complexation with metals but few have determined pK_a characterization procedures. For example, in [58], citrate's pK_a values are determined using a buffered mixture of perchloric acid and sodium perchlorate. However, this is not applicable to the enterobactin system because enterobactin needs to be added to methanol to be soluble in aqueous solution, and perchlorate is highly explosive when combined with organics.

Newer approaches in ITC allow pK_a to be calculated directly, but few literature papers were found in this regard [51]. In this approach, the reagent of unknown pK_a values is added all in a single injection to several solutions with different pH values. Plotting the

minima or maxima of the heat event versus pH results in a sigmoid curve where pK_a corresponds to the inflection point of the curve. The amplitude of the peaks from the heat events is proportional to the degree of dissociation. This can be expressed mathematically as the equation,

$$\left(\frac{dQ}{dt}\right)_{max,obs} = \left(\frac{dQ}{dt}\right)_{max,low} + \frac{\left(\frac{dQ}{dt}\right)_{max,high} - \left(\frac{dQ}{dt}\right)_{max,low}}{1+10^{(pKa-pH)}} \quad (5\text{-}1)$$

Based on this concept, a slightly modified method was developed to fit out needs in determining the pK_a values of enterobactin using a combination of ITC and potentiometry. In our method, enterobactin was not injected in a single time as a titrant but placed in the vessel in a concentration of 0.1 mM with 3% methanol and NaCl to keep ionic strength at 0.1 M. The total titrand volume was 750 µl and the reference and sample cells contained exactly the same solutions. The titrant was also kept at ionic strength of 0.1M using NaCl and was injected progressively in a total of 83 injections of 3 µl each, 249 µl total. The main component of the titrant was trisodium phosphate, a weak base that progressively shifted the pH of the titrand. In order to get a good range of pH, several experiments needed to be performed, only changing the concentration of trisodium phosphate in the syringe. Three sets of experiments were done ranging from pH 5 to pH 11 roughly using concentrations of 1 mM, 5mM and 25mM trisodium phosphate. It is worth pointing out that these experiments were only done from low to high pH to avoid acid-to-base catalyzed hydrolysis that enterobactin is known to undergo because its backbone ring incorporates ester linkages [76]. All experiments were done at 25 ºC. In these experiments the values for $\left(\frac{dQ}{dt}\right)$ were recorded in thermograms analogous to the ones shown in Chapter 4. The heat of dilution was corrected by running blank experiments and subtracting them

from the sample data.

Once the ITC experiment was done, the reference cell of the experiment, containing exactly the same solution as the sample cell, was placed in the potentiometric titrator inside the jacketed cell, with a stirring bar. The same titrant that was used in the ITC experiment was loaded in the potentiometer dosimeter and the same experiment was performed in the potentiometer. The temperature was kept at 25 ºC as the titrant was delivered in 3 µl injections up to a volume of 249 µl. The same experiment was performed in the potentiometer except that the variable measured this time was pH, and a pH value was recorded for each injection.

Once the calorimetry and potentiometry experiments were finished, it was necessary to match their data injection by injection. Since only one pH value was recorded per injection, it was necessary to unify the data produced by the calorimeter, since several $\left(\frac{dQ}{dt}\right)$ values were recorded per injection. For this purpose, the peak area per injection was exported, therefore allowing a unified value for calorimetry that could be matched to the corresponding pH for each injection. Although in [51], the plot is $\left(\frac{dQ}{dt}\right)$ versus pH, looking at Equation 5-1, if all the heats of reaction are integrated over time, then the equation would still remain related to pH and pK_a in the same manner. An inflection point in the heat flow Q versus pH curve, can therefore be determined as a pK_a value.

5.4 Results with ITC-potentiometric titrations

Four sets of experiments were done for titrant concentrations of 1, 5, 25 and 50 mM and each of them was analyzed statistically by performing triplicates of the same experiment. Figure 5-5 shows the experimental data with the corresponding error bars out

of triplicates. The data were normalized for concentration according to Equation 4-1.

As can be seen, a broad range of pH is covered with the four titrant concentrations although more data points are collected towards the end of each data set and less during the first injections of the experiments. This result benefitted the data treatment since the final injections seem to be the critical ones for inflection point determination.

Although some changes in slope can be evidently seen in Figure 5-5, the data were fitted to a sigmoidal curve using Equation 5-1 and the software Origin. This allowed to determine inflection points in the sigmoidal curves that, as discussed previously, correspond to pK_a values for enterobactin. Figure 5-6 shows this data fit.

After data fitting, three regions were identified in the full data set, each of them fitted to a different sigmoidal curve. The pH corresponding to the inflection point, can be identified as a pK_a value for enterobactin and in this case, inflection points were identified at 6.86 ± 0.02, 8.93 ± 0.03 and 11.50 ± 0.2. Table 5-1 shows a comparison between these values and the literature reported ones.

In these experiments, only one more species that could deprotonate or protonate as the titration progressed was involved, phosphate. In some cases the dilution experiments performed can account for other species deprotonating, but in this case this was not accounted for in the dilution experiments since phosphate was exactly the species used for enterobactin's deprotonation. For this reason, it is necessary to take into account phosphate's pK_a values that may be in the same region of interest as enterobactin's. Since phosphate has pK_a values of pK_{a1}= 1.46, pK_{a2} = 6.75 and pK_{a3} = 11.39 [54], only the last two values need to be taken into account for possible interferences in the inflection point determination.

With this knowledge, the first experimentally determined pK_a appears to be potentially merging the first two literature reported pK_a for enterobactin and it could also be influenced by pK_{a2} of phosphate. This would explain that these three values are seen in a bigger slope (the other two sigmoidal curves are less pronounced) instead of in three separated slopes, since they are only 0.75 pH units apart from each other.

The second experimentally determined pK_a is in good agreement with the reported value for enterobactin in the literature, the reported 8.55 and the experimental 8.93 only disagree by 4%.

Regarding the third experimentally determined pK_a, it could be another yet undetermined pK_a of enterobactin (since due to solubility and UV-Vis limitation issues previous experiments had not evaluated enterobactin at this pH) or it could also be the last pK_a of phosphate. To clarify, experiments at higher concentrations of titrant could be performed in the future to expand these studies.

Regarding other thermodynamically interesting information that could characterize this reaction, in Chapter 4 it was discussed that ITC experiments directly measured the heat and therefore information about the enthalpy could be easily extracted from those measures. Two ways are well known to extract enthalpy information, data fitting using HypΔH or peak area data treatment. In section 4.4, an example using citrate was discussed and the enthalpy values for this reaction were extracted using HypΔH. In order to do this, a model in HySS had to be previously developed where the experimental information and the overall constants β were input. For enterobactin, only three values have been reported to date, all of them are stepwise constants K (K_4, K_5 and K_6). In order to convert them to overall constants β_4, β_5 and β_6 and being able to use them in the HySS model, Equation 1-

20 can be applied. As can be seen in Equation 1-20, for this conversion the values of K_1, K_2 and K_3 are needed, and since those values are unknown, a HySS model could not be created.

A different approach for enthalpy calculations was then tried, peak area data treatment. The theoretical base of these calculations is that after the dilution heat is subtracted from the sample heat, an average of the first peaks of the reaction (when the molecule is fully protonated) and an average of the last peaks of the reaction (when the molecule is fully deprotonated) is taken and then these averages are subtracted from each other and the result should be the enthalpy of the reaction. To perform enthalpy calculations in this manner, the reaction needs to run to completion or it is necessary to ensure that only one deprotonation has taken place. Due to the complexity of the model in this study, this could not be ensured and therefore enthalpy could not be calculated.

In conclusion, some of the already reported pK_a values for enterobactin were successfully identified using a new methodology that combined two of the most common techniques for pK_a and complexation studies. Possible limitations of other methods such as UV-Vis spectrophotometry may be overcome by this method and new pK_a values or complexation constants may be determined using it.

Table 5-1. Experimental and reported pK_a values of enterobactin

Reported pK_a values [71]	Experimental pK_a values
6.0 ± 0.5	6.86 ± 0.02
7.5 ± 0.2	8.93 ± 0.03
8.55 ± 0.09	11.50 ± 0.2

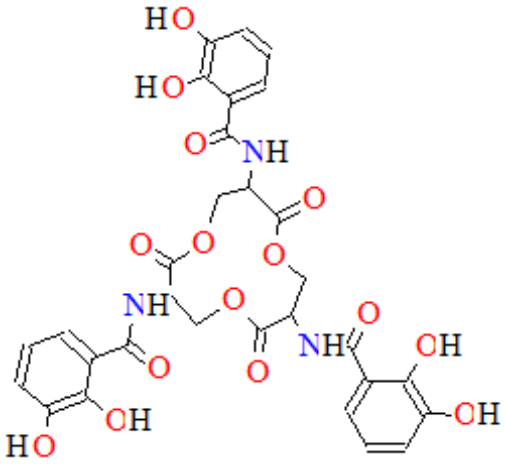

Figure 5-1. Enterobactin molecule view produced in structureview

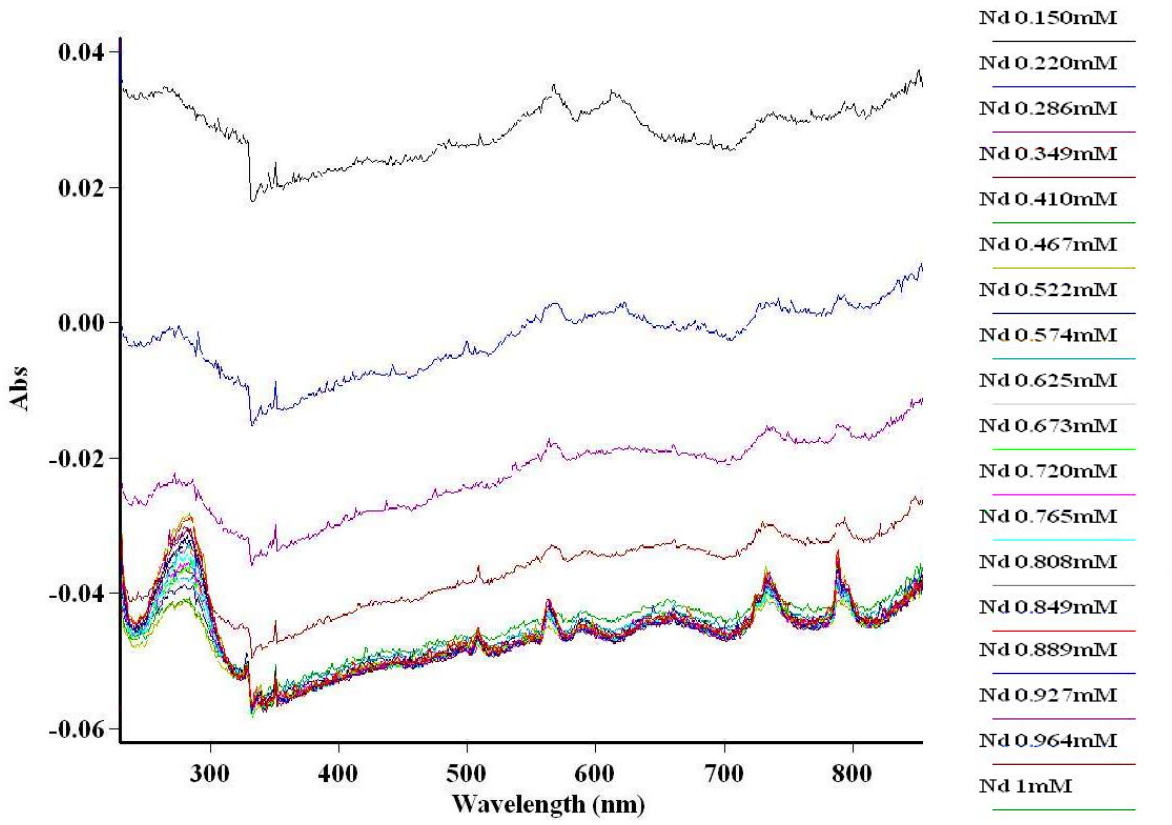

Figure 5-2. Neodymium signal trials in UV-Vis spectrophotometry

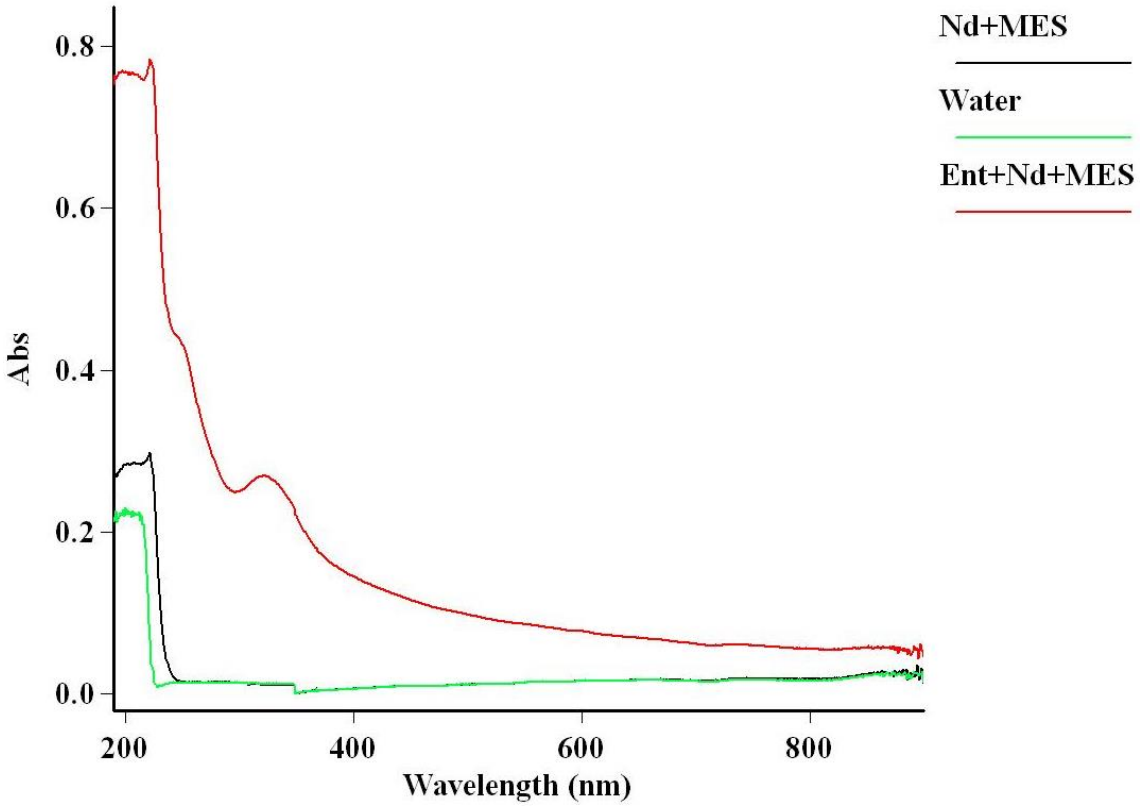

Figure 5-3. Enterobactin signal for complexation trials in UV-Vis spectrophotometry

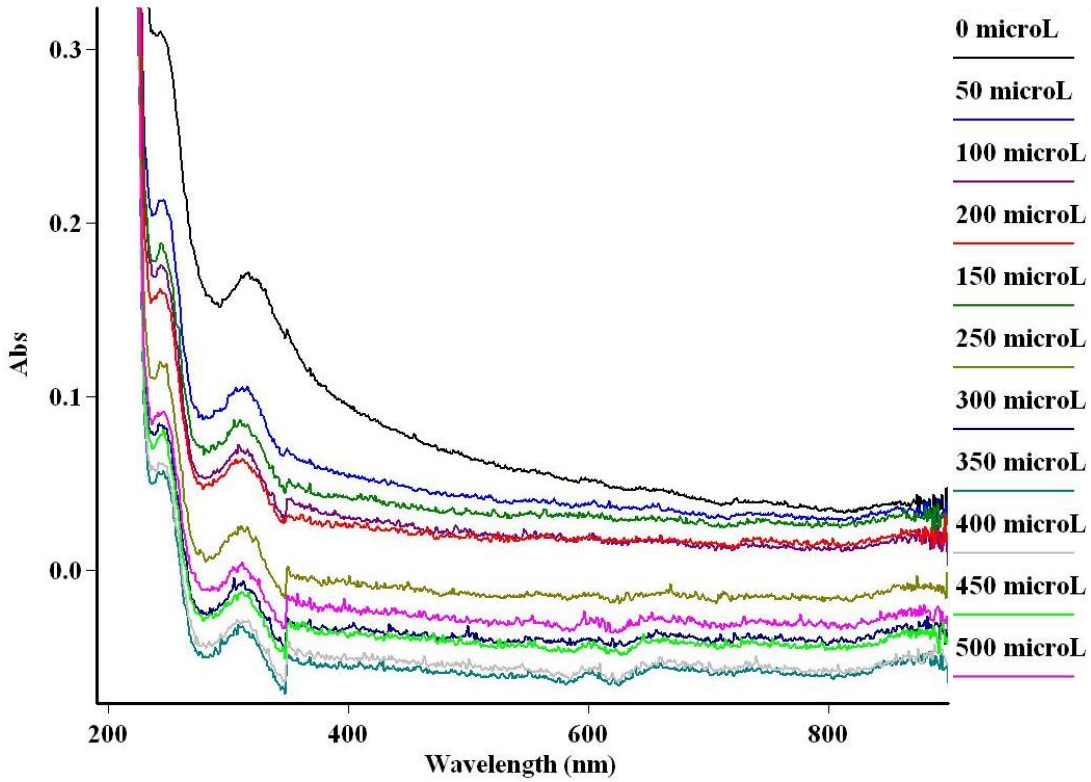

Figure 5-4. Ent-Nd complexation experiment in UV-Vis spectrophotometry

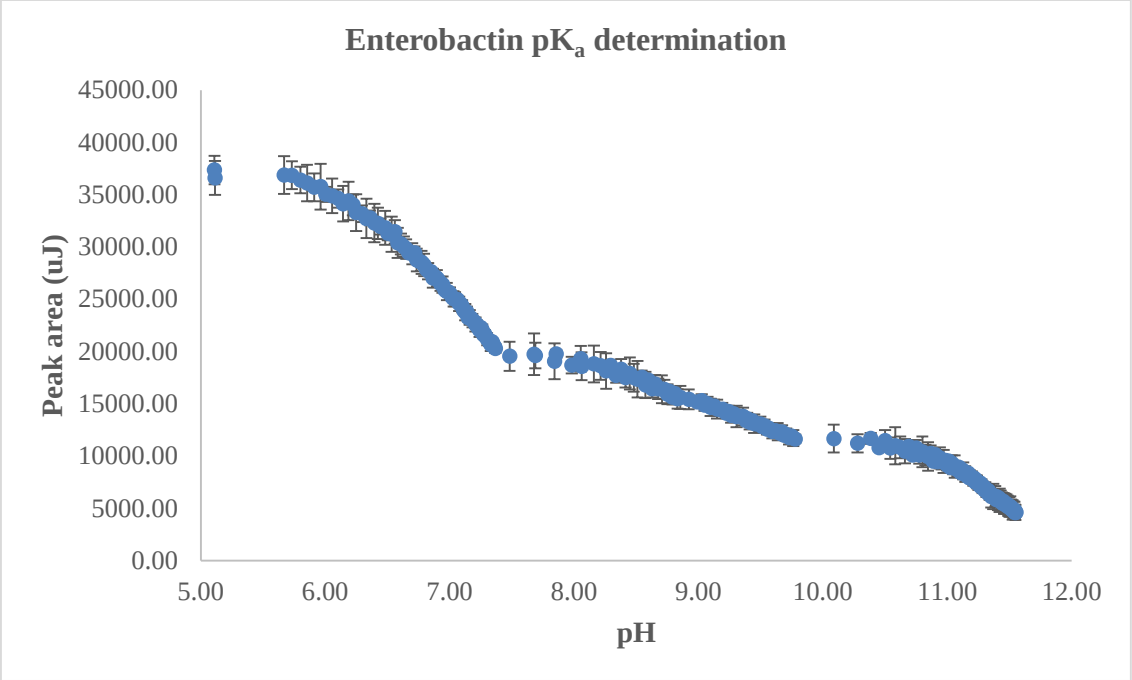

Figure 5-5. Enterobactin pK$_a$ determination with ITC-potentiometry

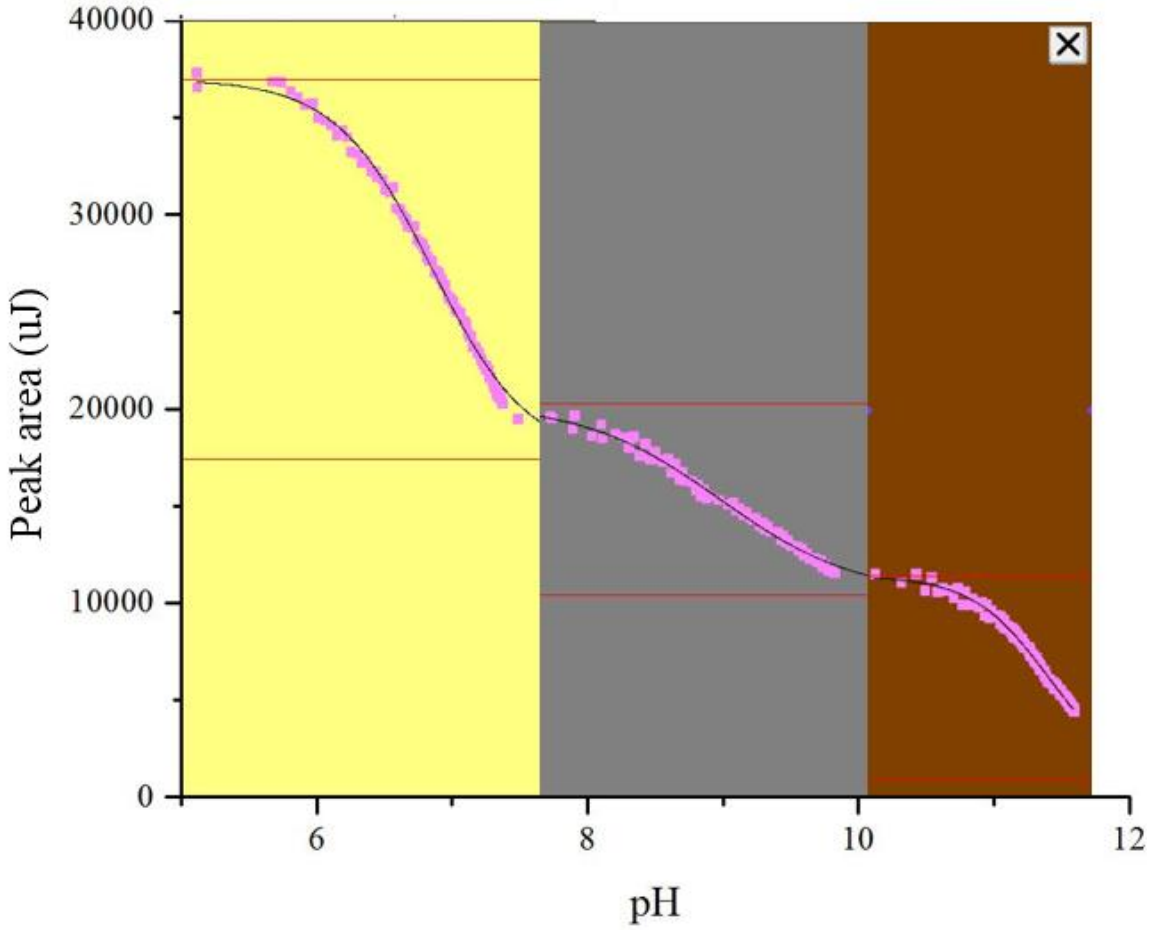

Figure 5-6. Data fit of enterobactin pK_a determination with ITC-potentiometry

CHAPTER 6

CONCLUSIONS

Enterobactin's potential to be a bioleaching ligand in uranium extraction was the main focus of this study. Its abundancy in nature and low pK_a values reported to date made it a great candidate for acid bioleaching. Relatively scarce information was available regarding enterobactin's complexation with trivalent metals and deprotonation constants. For this reason, fundamental studies were performed at a laboratory scale that could contribute to the characterization of enterobactin.

Although the ultimate metal of interest is uranium, to address the fact nuclear energy is a growing field with an increasing demand of fuel, working with uranium when performing fundamental studies is an unnecessary hazard. Choosing a lanthanide with a similar chemical behavior as uranium would eliminate the hazards of working with uranium, and therefore in this study the metal of choice was neodymium.

Three techniques were used in this study. The first one was UV-Vis spectrophotometry, since most of the reported work about enterobactin's complexation performed in other studies was done with this technique.

In previous work, enterobactin's UV-Vis signal was used to track the complexation of enterobactin with several trivalent metals, since those metals were not sensitive to UV-Vis light.

As a contrast, neodymium does have a UV-Vis signal, and therefore the complexation constants could potentially be determined from a shift in neodymium's signal or in enterobactin's. Since enterobactin's solubility limit is 0.1 mM, following a one-to-one stoichiometry, neodymium's signal was found to be too weak to see a shift that would allow stability constant determination, which lead to the use of enterobactin's signal to track the metal-ligand binding. An analog experiment to the ones previously performed with reported trivalent metals lead to no observable shifts in enterobactin's signal, likely due to the limitations in enterobactin's solubility and cell path length.

Potentiometric titrations were also considered for enterobactin's characterization after successfully testing the method with neodymium and citrate complexations. To be used individually, this technique needs rather large volumes to detect end points that would lead to stability constant determination, which in enterobactin's case was not possible due to its high added value.

The only available method remaining sensitive enough to detect changes with such small ligand concentrations is ITC. Only three out of nine pK_a values of enterobactin had been characterized to date, and although ITC had previously been used extensively for metal-ligand complexation studies, only a few papers were found containing methods for pK_a determination. None of the methods from the literature could be applied exactly to enterobactin, but enough information was extracted to design a new method suitable for the siderophore.

The new method consisted of a combination of ITC and potentiometric titrations and it was based on the fact that inflection points from a heat flow-pH curve could be related to pK_a values of the ligand though an analytical equation derived from the

Henderson-Hasselbach equation (Equation 1-9) and the relationship between heat flow and concentration of the sample.

In order to apply this method, the same experiment needs to be performed in both the calorimeter and the potentiometric titrator, at the same temperature, ionic strength and with the same concentrations. The number of injections and volume of titrant injected also needs to match exactly in order to relate point-by-point a pH value and a peak area corresponding to the same injection.

Four different sets of experiments were needed to cover a wide enough pH range that allowed the determination of several pK_a values. Triplicates were also done for statistical analysis and the data processing included a normalization according to Equation 4-1. Several trends were then identified in the total range of the obtained data and fitted to sigmoidal curves. With this information, several inflection points were then identified using analytical analysis and data fitting through Origin software.

Using this method, several pK_a values for enterobactin were identified. The results are in good agreement with the reported values from the literature and other potential pK_a values that have not been previously reported were also identified by overcoming some limitations that come with the use of a traditional method, such as cell path length in UV-Vis spectrophotometry.

The results from this work pave the way for potential applications of this technique to other ligand pK_a identification over a broad range of pH values that traditional techniques may not allow. The proficient use of the traditional approach to UV-Vis spectrophotometry could also be applied to other stability constant identification for different trivalent metals and enterobactin, such as gold, uranium or copper, although it did not produce positive

results for neodymium. Further studies of characterization of enterobactin could be done with the combined calorimetry-potentiometry method and would potentially enable strong enough evidence to use enterobactin as a ligand for bioleaching, whether it is for uranium extraction or heavy metal remediation.

REFERENCES

[1] OECD, NEA & IAEA, "Uranium 2014: Resources, production and demand," NEA, Paris, 2014.

[2] EPA, "Technologically enhanced naturally occurring radioactive materials from uranium mining volume 1: Mining and reclamation background," EPA, Washington D.C., 2008.

[3] C. Grey, "Uranium: From ore to concrete," *The Nuclear Engineer,* vol. 34, no. 1, 1993.

[4] K. Bosecker, "Bioleaching: Metal solubilization by microorganisms," *FEMS Microbiology Reviews,* no. 20, pp. 591-604, 1997.

[5] T. Rohwerder, T. Gehrke, K. Kinzler and S. W., "Bioleaching review part A: Progress in bioleaching: Fundamentals and mechanisms of bacterial metal sulfide oxidation," *Applied Microbiological Biotechnology,* no. 63, pp. 239-248, 2003.

[6] J. Muñoz, F. Gonzalez, M. Blazquez and A. Ballester, "A study of the bioleaching of a Spanish uranium ore. Part I: A review of the bacterial leaching in the treatment of uranium ores," *Hydrometallurgy* , no. 38, pp. 39-57, 1995.

[7] R. McCready and W. Gould, *Bioleaching of uranium*, New York: McGraw-Hill, 1990.

[8] G. J. Olson, J. A. Brierley and B. C. L., "Bioleaching review part B: Progress in bioleaching: Applications of microbial processes by the minerals industries," *Applied Microbiological Biotechnology,* no. 63, pp. 249-257, 2003.

[9] J. Munoz, A. Ballester, F. Gonzalez and M. Blazquez, "A study of the bioleaching of a Spanish ore. Part II: Orbital shaker experiments," *Hydrometallurgy,* no. 38, pp. 59-78, 1995.

[10] S. Hussien, O. Desouky, M. Abdel-Haliem and A. El-Mougith, "Uranium (VI) complexation with siderophores-pyoverdine produced by Pseudomans fluorescens SHA 281," *International Journal of Nuclear Energy Science and Engineering,* vol. 3, no. 4, pp. 95-102, 2013.

[11] L. Mullen, C. Gong and K. Czerwinski, "Complexation of uranium (VI) with the siderophore desferirioxamine B," *Journal of Radioanalytical and Nuclear Chemistry,* vol. 273, no. 3, pp. 683-688, 2007.

[12] R. Hider and X. Kong, "Chemistry and biology of siderophores," *Natural Product Reports,* no. 27, pp. 637-657, 2010.

[13] D. van der Helm and G. Winkelmann, "Hydroxamates and polycarboxylates as iron transport agents (siderophores) in fungi," in *Metal Ions in Fungi*, New York: Marcel Dekker, 1994, pp. 39-98.

[14] R. Hider, "Siderophore mediated absorption of iron," *Structure and Bonding,* no. 58, pp. 25-87, 1984.

[15] J. Renshaw, G. Robson, A. Trinci, M. Wiebe, F. Livens, D. Collison and R. Taylor, "Fungal siderophores: Structures, functions and applications," *Mycological Research,* vol. 10, no. 106, pp. 1123-1142, 2002.

[16] J. P. Day and P. Ackrill, "The chemistry of desferrioxamine chelation for aluminium overloadain renal dialysis patients," *Therapeutic Drug Monitoring,* no. 15, p. 598–601, 1993.

[17] G. Faa and G. Crisponi, "Iron chelating agents in clinical practice," *Coordination Chemistry Reviews,* vol. 184, p. 291–310, 1999.

[18] Y. Lu and M. J. Miller, "Syntheses and studies of multiwarhead siderophore-5-fluorouridine conjugates," *Bioorganic and Medicinal Chemistry,* vol. 7, p. 3025–3038, 1999.

[19] A. F. Vergne, A. J. Walz and M. J. Miller, "Iron chelators from mycobacteria (1954–1999) and potential therapeutic applications," *Natural Product Reports,* vol. 17, p. 99–116, 2000.

[20] M. Loyevsky, S. D. Lytton, B. Mester, J. Libman, A. Shanzer and Z. I. Cabantchik, "The antimalarial action of desferal involves a direct access route to erythrocytic (Plasmodium falciparum) parasites," *Journal of Clinical Investigation,* vol. 91, p. 218–224, 1993.

[21] G. N. Stradling, "Decorporation of actinides: A review of recent research," *Journal of Alloys and Compounds* , vol. 271/273, p. 72–77, 1998.

[22] E. D. Weinberg, "The role of iron in protozoan and fungal infectious diseases," *Journal of Eukaryotic Microbiology,* vol. 46, p. 231–238, 1999.

[23] M. Ledin and K. Pedersen, "The environmental impact of mine wastes – roles of microorganisms and their significance in treatment of mine wastes," *Earth Science*

Reviews, vol. 41, p. 67–108, 1996.

[24] S. N. Gray, "Fungi as potential bioremediation agents in soil contaminated with heavy or radioactive metals," *Biochemical Society Transactions,* vol. 26, p. 666–670, 1998.

[25] S. M. Kraemer, S. F. Cheah, R. Zapf, J. D. Xu, K. N. Raymond and G. Sposito, "Effect of hydroxamate siderophores on Fe release and Pb (II) adsorption by goethite," *Geochimica Et Cosmochimica Acta,* vol. 63, p. 3003–3008, 1999.

[26] U. Neubauer, B. Nowak, G. Furrer and R. Schulin, "Heavy metal sorption on clay minerals affected by the siderophore desferrioxamine B," *Environmental Science & Technology,* vol. 34, p. 2749–2755, 2000.

[27] J. R. Brainard, B. A. Strietelmeier, P. H. Smith, P. F. Langsten-Unkefer, M. E. Barr and R. R. Ryan, "Actinide binding and solubilization by microbial siderophores," *Radiochimica Acta,* vol. 58/59, p. 357–363, 1992.

[28] A. Gopalan, O. Zincircioglu and P. Smith, "Minimization and remediation of DOE nuclear waste problems using high selectivity actinide chelators," *Radioactive Waste Management and the Nuclear Fuel Cycle,* vol. 17, p. 161–175, 1993.

[29] B. J. Hernlem, L. M. Vane and G. D. Sayles, "The application of siderophores for metal recovery and waste remediation: Examination of correlations for prediction of metal affinities," *Water Research,* vol. 33, p. 951–960, 1999.

[30] S. G. John, C. E. Ruggiero, L. E. Hersman, C. S. Tung and M. P. Neu, "Siderophore mediated plutonium accumulation by microbacterium flavescens (JG-9)," *Environmental Science & Technology,* vol. 35, p. 2942–2948, 2001.

[31] R. J. Taylor, I. May, A. L. Wallwork, I. S. Denniss, N. J. Hill, B. Y. Galkin, B. Y. Zilberman and Y. S. Fedorov, "The applications of formo- and aceto-hydroxamic acids in nuclear fuel reprocessing," *Journal of Alloys and Compounds,* vol. 271, p. 534–537, 1998.

[32] I. S. Denniss and A. P. Jeapes, "Reprocessing irradiated fuel," in *The Nuclear Fuel Cycle: From ore to waste*, Oxford, UK: Oxford University Press, 1996, p. 116–137.

[33] R. Smith, A. Martell and R. Motekaitis, "Prediction of stability constants I. Protonation constants of carboxylates and formation constants of their complexes with class A metal ions," *Inorganica Chimica Acta,* no. 99, pp. 207-216, 1985.

[34] R. Smith, R. Motekaitis and A. Martell, "Prediction of stability constants II. Metal chelates of natural alkyl amino acids and their synthetic analogs," *Inorganica Chimica Acta,* no. 103, pp. 73-82, 1985.

[35] L. Alderighi, P. Gans, A. Ienco, D. Peters, A. Sabatini and V. A., "Hyperquad simulation and speciation (HySS): A utility program for the investigation of equilibria involving soluble and partially soluble species," *Coordination Chemistry Reviews,* no. 184, pp. 311-318, 1999.

[36] M. Eigen and K. Tamm, "Eigen-Tamm mechanism," *Electrochemistry,* vol. 66, no. 107, p. 93, 1962.

[37] A. Crumbliss and J. Harrington, "Iron sequestration by small molecules: Thermodynamic and kinetic studies of natural siderophores and synthetic model compounds," in *Advances in Inorganic Chemistry*, Elsevier, 2009, pp. 179-250.

[38] J. Reijenga, A. van Hoof, A. van Loon and B. Teunissen, "Development of methods for the determination of pK_a values," *Analytical Chemistry Insights,* no. 8, pp. 53-71, 2013.

[39] L. Benet and J. Goyan, "Potentiometric determination of dissociation constants," *Journal of Pharmaceutical Science,* vol. 56, p. 65–80, 1967.

[40] J. Saurina, S. Hernández-Cassou, R. Tauler and A. Izquierdo-Ridorsa, "Spectrophotometric determination of pK(a) values based on a pH gradient flow-injection system," *Analytica Chimica Acta,* vol. 408, no. 1-2, pp. 135-143, 2000.

[41] R. Gelb, "Conductometric determination of pK_a values. Oxalic and squaric acids," *Analitical Chemistry,* vol. 43, no. 8, p. 1110–3, 1971.

[42] I. Zimmerman, "Determination of pK_a values from solubility data," *International Journal of Pharmaceutics,* vol. 13, p. 57, 1982.

[43] S. Poole, S. Patel, K. Dehring, H. Workman and C. Poole, "Determination of acid dissociation constants by capillary electrophoresis," *Journal of Chromatography A,* vol. 1037, no. 1-2, p. 445–454, 2004.

[44] C. Golumbic, M. Orchin and S. Weller, "Relation between partition coefficient and ionization constant," *Journal of American Chemical Society,* vol. 71, pp. 2624-2627, 1949.

[45] K. Popov, H. Rönkkömäki and L. Lajunen, "Guidelines for NMR measurements for determination of high and low pK_a values (IUPAC Technical Report)," *Pure and Applied Chemistry,* vol. 78, no. 3, p. 663–675, 2006.

[46] L. Katzin and E. Gulyas, "Dissociation constants of tartaric acid with the aid of polarimetry," *Journal of Physical Chemistry,* vol. 64, pp. 1739-1741, 1960.

[47] W. J. Barette, H. J. Johnson and D. Sawyer, "Voltammetric evaluation of the effective acidities (pK_a) for Brönsted acids in aprotic solvents," *Journal of American Chemical*

Society, vol. 56, p. 1890, 1984.

[48] J. Bunnett and N. Nudelman, "An independent kinetic method for determining acid dissociation constants in methanol," *Journal of Organic Chemistry,* vol. 34, p. 2043, 1969.

[49] R. Singhal and W. Cohn, "Cation-exclusion chromatography on anion exchangers: Application to nucleic acid components and comparison with anion-exchange chromatography," *Biochemistry,* vol. 12, no. 8, pp. 1532-1537, 1973.

[50] L. Rosenberg, J. Simons and S. Schulman, "Determination of pK_a values of N-heterocyclic bases by fluorescence spectrophotometry," *Talanta,* vol. 26, no. 9, pp. 867-871, 1979.

[51] S. Tajc, B. Tolbert, R. Basavappa and B. Miller, "Direct determination of thiol pK_a by isothermal titration microcalorimetry," *Journal of American Chemical Society,* vol. 126, pp. 10508-10509, 2004.

[52] L. Xing, R. Glen and R. Clark, "Predicting pK(a) by molecular tree structured fingerprints and PLS," *Journal of Chemical Information and Computer Science,* vol. 43, no. 3, pp. 870-879, 2003.

[53] P. Gans, A. Sabatini and A. Vacca, "Investigation of equilibria in solution. Determination of equilibrium constants with the HYPERQUAD suite of programs," *Talanta,* no. 43, pp. 1739-1753, 1996.

[54] L. Pettit, "IUPAC stability constants database," *Chemistry International,* vol. 28, no. 5, pp. 14-15, 2009.

[55] P. Gans and B. O'Sullivan, "GLEE, a new computer program for glass electrode calibration," *Talanta,* no. 51, pp. 33-37, 2000.

[56] F. Rossotti and H. Rossotti, "Potentiometric titrations using Gran plots," *Journal of Chemical Education,* vol. 42, no. 7, pp. 375-378, 1965.

[57] A. Vogel, *Vogel's textbook of quantitative inorganic analysis,* Longman, 1961.

[58] M. Brown, A. Kropf, A. Paulenova and A. Gelis, "Aqueous complexation of citrate with neodymium (III) and americium (III): A study by potentiometry, absorption spectrophotometry, microcalorimetry, and XAFS," *Dalton Transactions,* no. 43, pp. 6446-6454, 2014.

[59] P. Vanysek, "The glass pH electrode," *The Electrochemical Society Interface,* vol. Summer, pp. 19-20, 2004.

[60] C. Haider, "Electrodes in potentiometry," Metrohm Ltd: Herisau, 2004.

[61] D. Skoog, D. West and F. Holler, *Analytical chemistry: An introduction (Saunders Golden Sunburst Series)*, 7th ed.: Cengage Learning, 1999.

[62] D. A. Skoog, D. M. West, F. J. Holler and S. Crouch, *Fundamentals of analytical chemistry*, 8th ed.: Brooks Cole, 2003.

[63] Gilchrist, J.R.; Gilden Photonics Ltd., "Spectroscopy: The tools of the trade," in *Photonics spectra handbook*, Pittsfield: Laurin Publishing Company, Inc..

[64] Varian, Inc., "Cary 100, 300 UV-Vis spectrophotometers specification sheet," Varian, Inc., Australia, 2006.

[65] Hamamatsu Photonics K.K., "Chapter 14. Applications," in *Photomultiplier tubes. Basics and applications*, Japan: Hamamatsu Photonics K.K., 2007, pp. 266-304.

[66] J. D. J. Ingle and S. R. Crouch, *Spectrochemical analysis*, New Jersey: Prentice Hall, 1988.

[67] K. Takacs-Novak and K. Tam, "Multiwavelength spectrophotometric determination of acid dissociation constants: A validation study," *Analytica Chimica Acta*, vol. 434, pp. 157-167, 2001.

[68] T. Moeller and J. Brantley, "Observations on the rare earths. LVIII. Reaction between neodymium and ethylenediaminetetraacetate ions in aqueous solution," *Journal of American Chemical Society*, vol. 72, no. 12, p. 5447–5451, 1950.

[69] B. Sivasankar, "Molecular spectroscopy," in *Engineering Chemistry*: McGraw-Hill, 2008, p. 299.

[70] K. Raymond, E. Dertz and S. Kim, "Enterobactin: An archetype for microbial iron transport," *Proceedings of the National Academy of Sciences*, vol. 100, no. 7, pp. 3584-3588, 2003.

[71] L. Loomis and K. Raymond, "Solution equilibria of enterobactin and metal-enterobactin complexes," *Inorganic Chemistry*, vol. 30, pp. 906-911, 1991.

[72] G. O'Brien and F. Gibson, "The structure of enterochelin and related 2,3-dihydroxy-N-benzoylserine conjugates from Escherichia coli," *Biochimica et Biophysica Acta*, vol. 215, no. 2, pp. 393-402, 1970.

[73] J. Telford and K. Raymond, "Coordination chemistry of the amonabactins, bis(catecholate) siderophores from Aeromonas hydrophila," *Inorganic Chemistry*, vol. 37, pp. 4578-4583, 1998.

[74] R. Scarrow, D. Ecker, C. Ng, S. Liu and K. Raymond, "Iron (III) coordination chemistry of linear dihydroxyserine compounds derived from enterobactin,"

Inorganic Chemistry, vol. 30, pp. 900-906, 1991.

[75] W. Harris, C. Carrano, S. Cooper, S. Sofen, A. Avdeef, J. McArdle and K. Raymond, "Coordination chemistry of microbial iron transport compounds. 19. Stability constants and electrochemical behavior of ferric enterobactin and model complexes," *Journal of American Chemical Society,* vol. 101, pp. 6097-6104, 1979.

[76] K. Greenwood and R. Luke, "Enzymatic hydrolysis of enterochelin and its iron complex in Escherichia coli K-12. Properties of enterochelin esterase," *Biochimica Biophysica Acta,* vol. 525, p. 209, 1978.

[77] Skoog et al., in *Principles of instrumental analysis*, Belmont, CA: Thomson Brooks/Cole, 2007, pp. 169-173.